CHARPTER IV

RESULTS & DISCUSSION

Artemisinin and its derivatives are candidates for antimalarial and anticancer drugs. However, artemisinin and its derivatives also have the limitation to be the effective drugs due to their low solubility in water or oil, and thus can only be administered orally. Moreover, arteether and artemether have been reported to cause neurotoxicity.[98,52] Furthermore, C-10 acetal (C-O) types deoxoartemisinin derivatives such as dihydroartemisinin, arteether and artelinic acid are less hydrolytically stable than artemisinin. On the other hand, C-10 non acetal (C-C) types deoxoartemisinin derivatives such as 10-(n-butyl)-deoxoartemisinin and 10-benzyldeoxoartemisinin are more hydrolytically stable than C-10 acetal (C-O) types artemisinin derivatives under simulated stomach acid (pH = 2.0, 37 ^{o}C).[53] In addition, C-10 non-acetal (C-C) types deoxoartemisinin derivatives such as deoxoartemisinin analogs are readily absorbable by the gastrointestinal tract to provide the highest degree of bioavailability of the drug to a malaria patient and is therapeutically effective in smaller dosage units.[99] In a recent report, it has been revealed that the extent of antimalarial activity depends upon the extent the number of peroxide units, which can be increased by adding of additional artemisinin moiety through careful chemical manipulations.[78,77,76,10] In addition, the use of a peptide nucleic acid (PNA), a repeating unit of *N*-(2-aminoethyl) glycine (aeg) monomer, has proven to be powerful in molecular biology, diagnostic tools, and antisense therapeutics. These findings lead us to design and synthesis of C-10 non-acetal deoxoartemisinin pseudo peptide backbone compounds. It was thought that C-10 non-acetal deoxoartemisinin pseudo peptide backbone compounds

may show interesting bioactivities that could be applied for medicinal use such as antimalarial, anticancer, and other biological activities.

4.1 Synthesis of Fmoc-aeg-deoxoartemisinin-*t*Bu oligomers

The synthesis of Fmoc-aeg-deoxoartemisinin-*t*Bu oligomers could be acheived from fully blocked artemisinin monomer **9** by using typical sequential deprotection–coupling steps in peptide synthesis. The requisite monomers **132** can be prepared from reaction of deoxoartemisinin and *N*-(2-aminoethyl) glycine (**133**) as shown in Scheme 4.1. Carboxylic acid precursor **131** could be obtained from the oxidation of allyl **130**. The key intermediate, 10β-allyldeoxoartemisinin had been previously synthesized by treatment of dihydroartemisinin 10α-benzoate (**129**) with allyltrimethylsilane using catalytic lewis acid such as zinc chloride.[77,78,100]

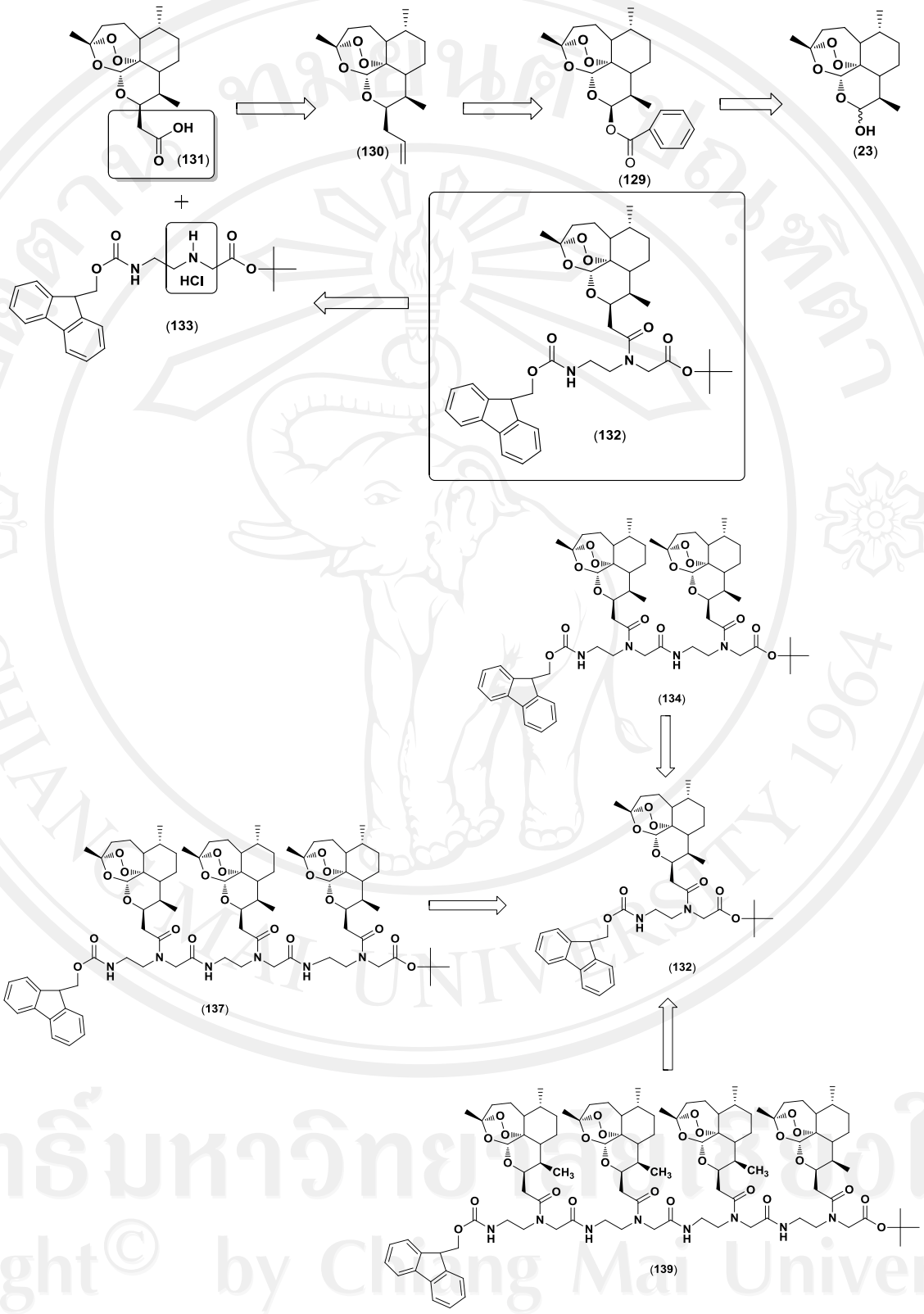

Scheme 4.1 Retrosynthesis of Fmoc-aeg-deoxoartemisinin-*t*Bu oligomers.

4.1.1 Preparation of 10β-Carboxylalkyldeoxoartemisinin (131)

Dihydroartemisinin (**23**) was synthesized according to the previous procedure described in the literature.[101] Briefly, dihydroartemisinin was benzoylated by using benzoyl chloride in the presence of pyridine and purified by flash column chromatrography (Scheme 4.2). This reaction went smoothly to give dihydro-artemisinin 10α-benzoate (**129**) as a white solid in good yields (85%).

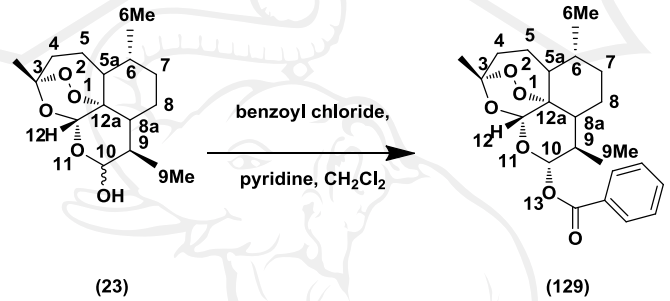

Scheme 4.2 Synthesis of dihydroartemisinin 10α-benzoate. (**129**)

^{1}H NMR, IR and MS data were in good agreement with those reported for the benzoyl derivative. The aromatic protons of phenyl group showed two protons doublet peaks at 8.13 ppm (2H, m, Ar-H), 7.61 ppm (1H, m, Ar-H) and 7.45 ppm (2H, m, Ar-H). The signal of one proton doublet peaks at 6.02 ppm (1H, d, J = 10 Hz) accounted for the proton H-10. The signal of one proton singlet peak at 5.53 ppm (s, 1H) was assigned for H-12, while the signal at δ 2.76 ppm (1H, sextet) was accounted for H-9. The signal of three protons doublet peaks at δ 0.99 ppm (3H, d, J = 6.06 Hz) and δ 0.93 ppm (3H, d, J = 7.14) were assigned for proton 6-Me and 9-Me, respectively (Appendix IV). The rest of protons were similar to artemisinin ring such as 2.40 ppm (1H, td, J = 13.59, 3.98 Hz, H-4), 2.05 ppm (1H, m, H-4), 1.90 (1H, m, H-5), 1.85-1.76 ppm (3H, m, H-8, H-7, H-8a), 1.47 ppm (1H, m, H-5), 1.43 ppm (3H, s, 3-Me), 1.40-1.30 ppm (2H, m, H-5a, H-6) and 1.10-1.08 ppm (2H, m, H-8, H-7).[102]

ESI mass spectrometry showed molecular ion peak at 411.1784 correspond to $[M+Na]^+$ (Appendix II). The compounds showed IR absorption at 3037 ($\upsilon_{=C-H}$, aromatic), 2928 (υ_{C-H}, alkane), 1736 ($\upsilon_{C=O}$, ester), 1584 ($\upsilon_{C=C}$, aromatic), 1452 ($\upsilon_{C=C}$, aromatic), 1377 (δ_{C-H}, alkane), 1273 ($\upsilon_{C-C(O)-C}$, ester), 1037, 877 (O-O) and 831 (O-O), 714 (δ_{C-H}, aromatic) cm^{-1} (Appendix III).

Allylation of 10α-benzoate **129** with allyltrimethylsilane using zinc chloride as lewis acid catalyst in anhydrous 1,2-dichloroethane gave the mixture of α and β allyl compounds (Scheme 4.3). The mixture was separated by column chromatography to give 10β-allyldeoxoartemisinin (**130**) in moderate yields (69%).

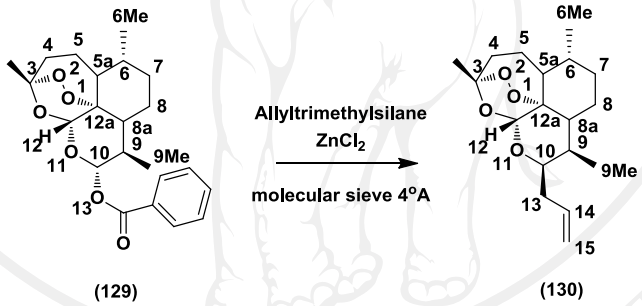

Scheme 4.3 Synthesis of 10β-allyldeoxoartemisinin. (**130**)

^{1}H NMR and IR data were in good agreement with those reported for the allyl derivative. The signal of one proton singlet peak at δ 5.33 ppm was accounted for the proton H-12, while the two protons signals at δ 5.9 ppm (1H, m) and δ 5.1 ppm (2H, m) were assigned for proton H-14 and H-15, respectively. The one proton of the H-10β and H-9 appeared at δ 4.31 ppm (1H, m) and 2.68 ppm (1H, sextet, J = 7.2 Hz), respectively. The chemical shift of H-13 was approximately between δ 2.45-2.17 ppm as multiplet pattern. The signal of one proton at δ 2.35 ppm (1H, td, J = 13.75, 4 Hz) was accounted for the proton H-4. The signal of three protons doublet peaks at δ 0.99

ppm (3H, d, J = 5.89 Hz) and δ 0.93 ppm (3H, d, J = 7.57) were assigned for proton 6-Me and 9-Me, respectively. The rest of protons were similar to artemisinin ring of dihydroartemisinin 10α-benzoate (**129**) (Appendix IV). The compounds showed IR absorption at IR (KBr) 3074 ($\upsilon_{=C-H}$, alkene), 2929 (υ_{C-H}, alkane), 1642 ($\upsilon_{C=C}$, alkene), 1455 (δ_{CH2}, alkane), 1377 (δ_{CH3}, alkane), 1002 ($\delta_{oop-C=C-H}$, alkene), 924 ($\delta_{oop-C=C-H}$, alkene), 880 (O-O) and 839 (O-O) cm^{-1} (Appendix III).

Finally, the corresponding carboxylic acid **131** was acheived by using $NaIO_4/KMnO_4$ at room temperature to obtain 10β-carboxylalkyldeoxoartemisinin (**131**) in good yield (80%) as shown in scheme 4.4.

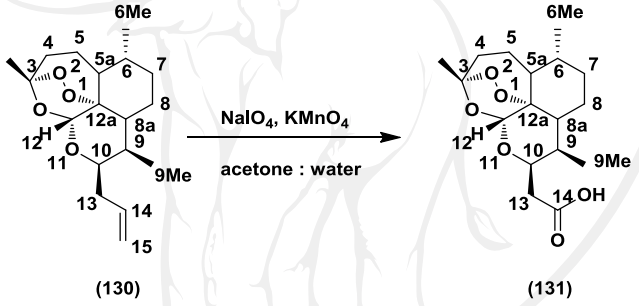

(130) (131)

Scheme 4.4 Synthesis of 10β-carboxylalkyldeoxoartemisinin. (**131**)

^{1}H NMR and IR data were in good agreement with those reported for the carboxylic acid derivative. The signal of one proton singlet peak at δ 5.40 ppm accounted for the proton H-12 (1H, s), while the signals at δ 4.85 ppm (1H, ddd, J = 9.9, 6.3, 3.9 Hz) were assigned for proton H-10β. The chemical shift of H-9 and H-13 were approximately between δ 2.80-2.49 ppm as multiplet pattern. The signal of one proton at δ 2.34 ppm (1H, td, J = 13.94, 3.91 Hz) was assigned for proton H-4. The signal of three protons doublet peaks at δ 0.99 ppm (3H, d, J = 5.78 Hz) and δ 0.93 ppm (3H, d, J = 7.20) were assigned for proton 6-Me and 9-Me, respectively. The rest of protons were similar to artemisinin ring of dihydroartemisinin 10α-benzoate (**129**)

(Appendix IV). The compounds showed IR absorption at 2953 (υ_{C-H}, alkane), 2874 (υ_{C-H}, alkane), 1715 ($\upsilon_{C=O}$, carboxylic acid), 1455(δ_{CH2}, alkane), 1385 (δ_{CH3}, alkane), 1209 (υ_{C-O}, carboxylic acid), 1113, 1011, 948 (δ_{oop}, O-H) and 878 (O-O) cm^{-1} (Appendix III).

4.1.2 Synthesis of Fmoc-aeg-deoxoartemisinin-*t*Bu monomer (**132**)

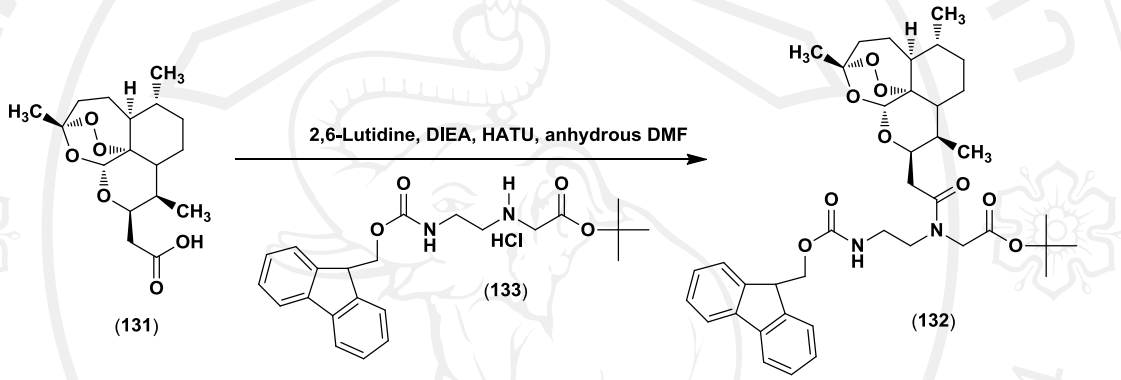

Scheme 4.5 Synthesis of Fmoc-aeg-deoxoartemisinin-*t*Bu monomer. (**132**)

Fmoc-aeg-deoxoartemisinin-*t*Bu monomer (**132**) was prepared by coupling 10β-carboxylalkyldeoxoartemisinin (**131**) to *tert*-butyl *N*-[2-(*N*-9-fluorenylmethoxy-carbonyl) aminoethyl] glycinate hydrochloride (**133**) using HATU as coupling agent. After purification by flash column chromatography afforded the desired product as a white solid in excellent yields (91%). The product was further purified by RP-HPLC using a C18 column running a gradient of acetonitrile. Major peak was collected and analysed by MS. ESI mass spectrometry showed molecular ion peak at 727.3567 correspond to $[M+Na]^+$ (Appendix II). In addition, the compound showed IR absorption at 3412 (υ_{N-H}, amide), 3062 ($\upsilon_{=C-H}$, aromatic), 2938 (υ_{C-H}, alkane), 2874 (υ_{C-H}, alkane), 1720 ($\upsilon_{C=O}$, ester), 1644 ($\upsilon_{C=O}$, amide), 1513 ($\upsilon_{C=C}$, aromatic), 1450 ($\upsilon_{C=C}$, aromatic), 1370 (δ_{CH3}, alkane), 1231 ($\upsilon_{C-C(O)-C}$, ester), 1154, 877 (O-O) and 739 (δ_{C-H}, aromatic) cm^{-1} (Appendix III). The NMR spectrum showed two rotamers : 6.10

(1/2H, br, rotamer, NH), 5.90 (1/2H, br, rotamer, NH), 5.35 (1/2H, s, rotamer, H-12), 5.30 (1/2H, s, rotamer, H-12), 5.00-4.90 (1/2H, m, rotamer, H-10), 4.72-4.65 (1/2H, m, rotamer, H-10), 4.42 (1/2H, m, rotamer, H-22), 4.39 (1/2H, m, rotamer, H-22), 4.29 (1/2H, m, rotamer, H-22), 4.25 (1/2H, m, rotamer, H-22), 4.21 (1/2H, m, rotamer, H-23), 4.20 (1/2H, m, rotamer, H-23), 4.25 (1/2H, m, rotamer, H-19), 4.22 (1/2H, m, rotamer, H-19), 3.70 (1/2H, m, rotamer, H-19), 3.66 (1/2H, m, rotamer, H-19), 4.37 (1/2H, m, rotamer, H-16), 4.31 (1/2H, m, rotamer, H-16), 3.79 (1/2H, m, rotamer, H-16), 3.75(1/2H, m, rotamer, H-16), 1.50 (9H, s, rotamer, H-13), 1.48 (9H, s, rotamer, H-13) (Appendix IV).

4.2 Synthesis of Fmoc-aeg-deoxoartemisinin-*t*Bu oligomers

Synthesis of Fmoc-aeg-deoxoartemisinin-*t*Bu oligomers were synthesized *via* peptide coupling reaction by coupling the carboxyl group or C-terminus of monomer or other oligomers acid to the amino group or N-terminus of another molecule.

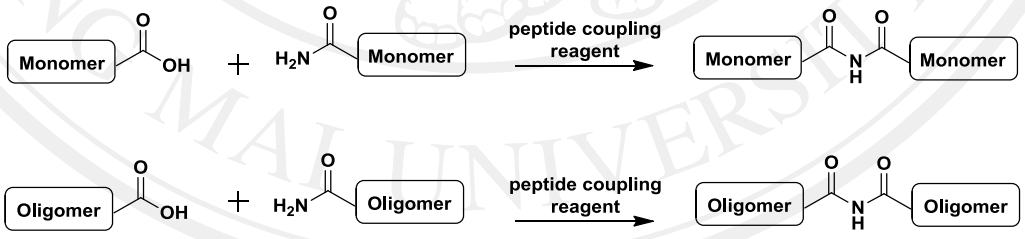

Scheme 4.6 Synthesis pathway of peptide synthesis.

4.2.1 Synthesis of Fmoc-aeg-deoxoartemisinin-*t*Bu dimer (134)

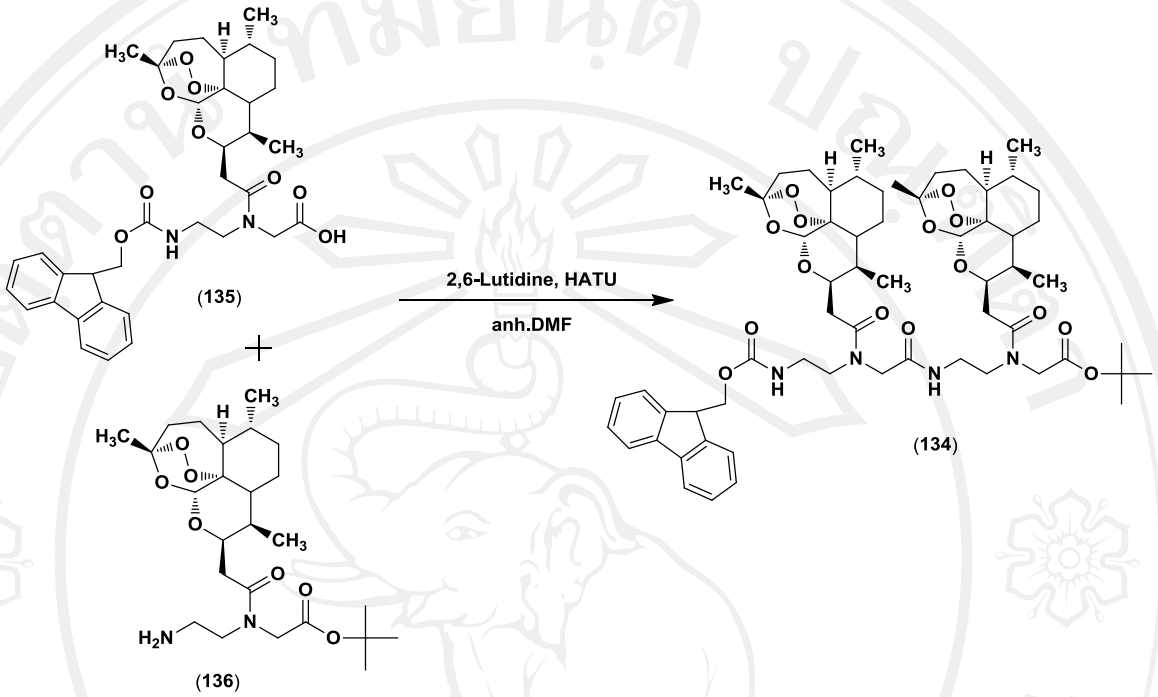

Scheme 4.7 Synthesis of Fmoc-aeg-deoxoartemisinin-*t*Bu dimer. (**134**)

Fmoc protecting group of Fmoc-aeg-deoxoartemisinin-*t*Bu monomer (**132**) was removed under basic condition using 20% piperidine in DMF to afford NH_2-aeg-deoxoartemisinin-*t*Bu monomer (**136**). This reaction went smoothly to give the desired product in good yield (91%). Deprotection of Fmoc-aeg-deoxoartemisinin-*t*Bu monomer (**132**) was acheived by using trifluoroacetic acid in anhydrous dichloromethane to provide Fmoc-aeg-deoxoartemisinin-OH monomer (**135**). Coupling of NH_2-aeg-deoxoartemisinin-*t*Bu monomer (**136**) with Fmoc-aeg-deoxoartemisinin-OH monomer (**135**) was performed by HATU as the coupling agent in the presence of 2,6-lutidine in DMF. The reaction proceeded very smoothly affording the desired dimer in good yield (88%) (Scheme 7). ESI mass spectrometry showed molecular ion peak at 1135.6098 correspond to $[M+Na]^+$ (Appendix II). In addition, the compound showed IR absorption at 3369 (υ_{N-H}, amide), 3062 ($\upsilon_{=C-H}$,

aromatic), 2938 (υ_{C-H}, alkane), 2870 (υ_{C-H}, alkane), 1720 ($\upsilon_{C=O}$, ester), 1651 ($\upsilon_{C=O}$, amide), 1520 ($\upsilon_{C=C}$, aromatic), 1451 ($\upsilon_{C=C}$, aromatic), 1376 (υ_{CH3}, alkane), 1152 ($\upsilon_{C-C(O)-C}$, ester), 878 (O-O) and 741 (δ_{C-H}, aromatic) cm^{-1} (Appendix III).

4.2.2 Synthesis of Fmoc-aeg-deoxoartemisinin-*t*Bu trimer (137)

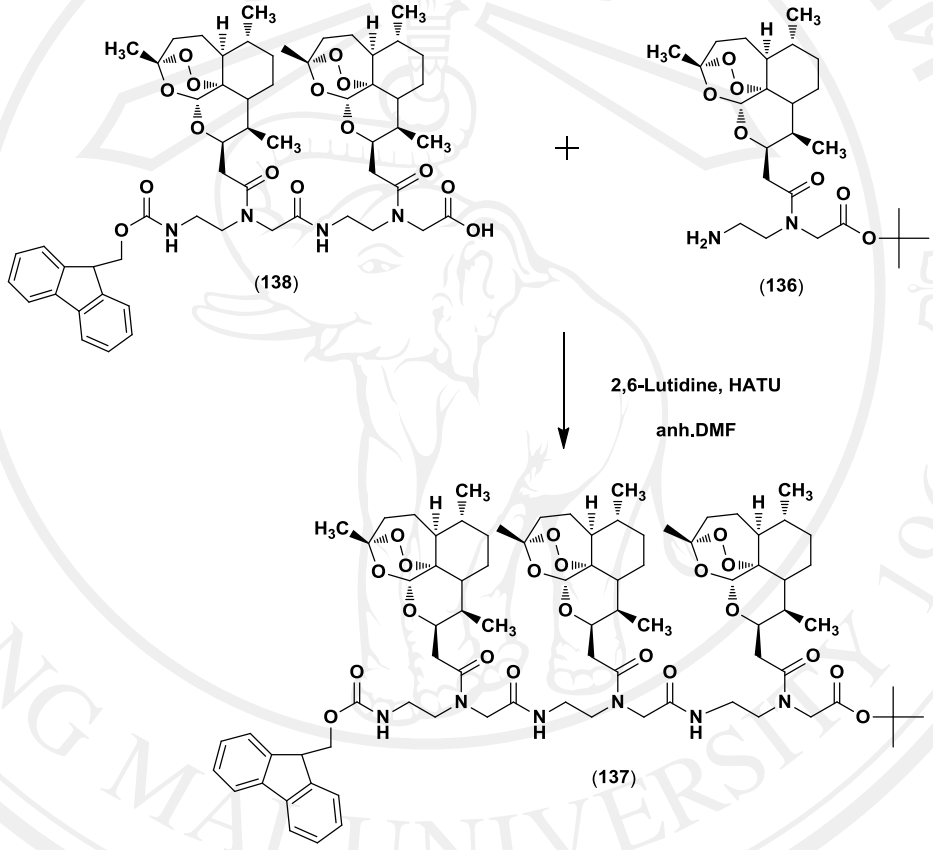

Scheme 4.8 Synthesis of Fmoc-aeg-deoxoartemisinin-*t*Bu trimer. (**137**)

Deprotection of *t*-Boc of dimer **134** by using TFA/CH_2Cl_2 gave acid **138**. Coupling of amino **136** to acid **138** using HATU as the coupling agent in the presence of 2,6-lutidine in DMF led to trimer **137** in moderate yield (73%) (Scheme 4.8). ESI mass spectrometry showed molecular ion peak at 1521.939 correspond to $[M+H]^+$ (Appendix II). The compound showed IR absorption at 3445 (υ_{N-H}, amide), 2926 (υ_{C-H}, alkane), 1644 ($\upsilon_{C=O}$, amide), 1541 ($\upsilon_{C=C}$, aromatic), 1451 ($\upsilon_{C=C}$, aromatic), 1371

(υ_{CH3}, alkane), 1211 ($\upsilon_{C\text{-}C(O)\text{-}C}$, ester), 877 (O-O) and 749 ($\delta_{C\text{-}H}$, aromatic) (Appendix III).

4.2.3 Synthesis of Fmoc-aeg-deoxoartemisinin-*t*Bu tetramer (139)

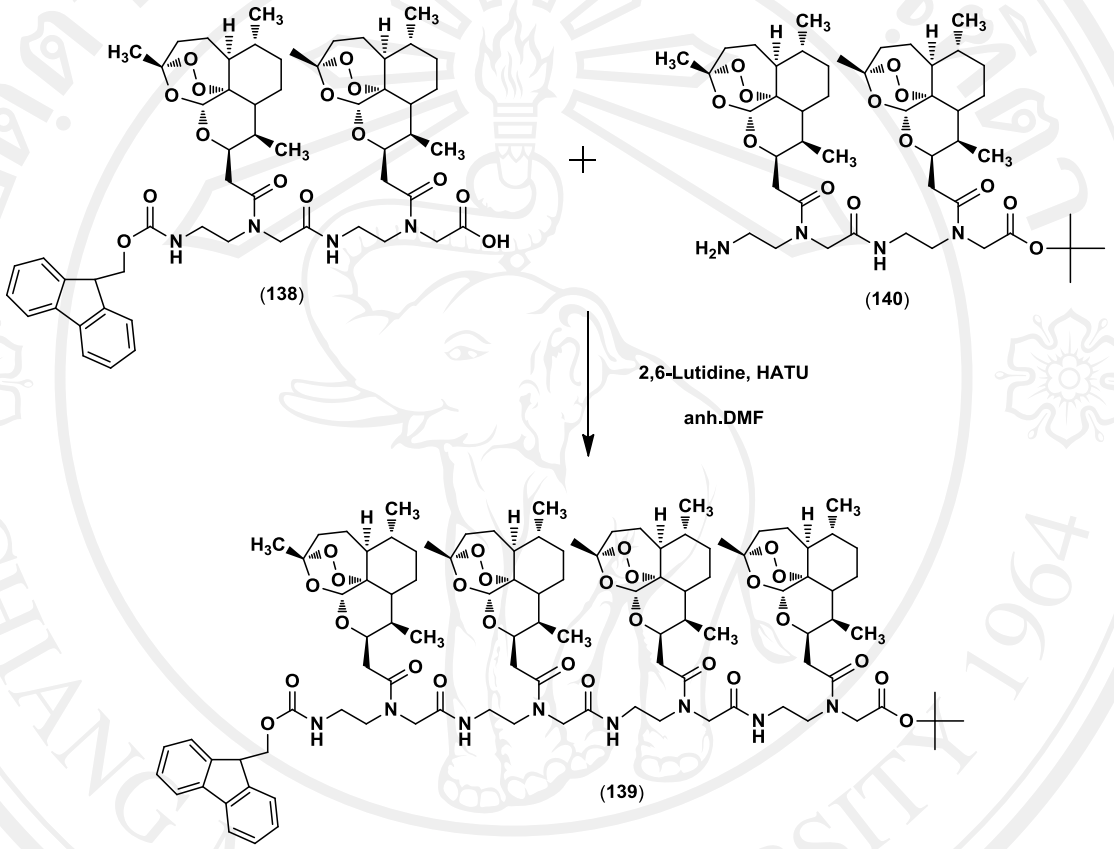

Scheme 4.9 Synthesis of Fmoc-aeg-deoxoartemisinin-*t*Bu tetramer. (**139**)

Fmoc-aeg-deoxoartemisinin-*t*Bu tetramer (**139**) was synthesized from coupling of NH_2-aeg-deoxoartemisinin-*t*Bu dimer (**140**) with Fmoc-aeg-deoxoartemisinin-OH dimer (**138**) by using standard coupling protocol (Scheme 8). Thus, Fmoc-group of Fmoc-aeg-deoxoartemisinin-*t*Bu dimer (**134**) was removed under basic condition (20% piperidine in DMF) to give NH_2-aeg-deoxoartemisinin-*t*Bu dimer (**140**). Coupling of NH_2-aeg-deoxoartemisinin-*t*Bu dimer (**140**) with Fmoc-aeg-deoxoartemisinin-OH monomer (**138**) was performed by using HATU as the coupling agent in the presence of 2,6-lutidine in DMF. After the reaction was

completed, the crude product was purified by flash chromatography to afford the desired tetramer **139** in moderate yields (60%). ESI mass spectrometry showed molecular ion peak at 1930.31 correspond to $[M+H]^+$ (Appendix II). The compound showed IR absorption at 3382 (υ_{N-H}, amide), 3063 ($\upsilon_{=C-H}$, aromatic), 2950 (υ_{C-H}, alkane), 1716 ($\upsilon_{C=O}$, ester), 1651 ($\upsilon_{C=O}$, amide), 1530 ($\upsilon_{C=C}$, aromatic), 1455 ($\upsilon_{C=C}$, aromatic), 1385 (υ_{CH3}, alkane), 1211 ($\upsilon_{C-C(O)-C}$, ester), 1155, 1138, 1107, 963, 886 (O-O) and 736 (δ_{C-H}, aromatic) (Appendix III).

4.3 Synthesis of Lysine-aeg-deoxoartemisinin-*t*Bu oligomers

Lysine amino acid was added to N-terminus of Fmoc-aeg-deoxoartemisinin-*t*Bu oligomers to observe the effect of lysine to the biological activity of Fmoc-aeg-deoxoartemisinin-*t*Bu oligomers. The fully protected lysine, Fmoc-lys(Boc)-OH (**142**) was used as a starting material and coupling with NH_2-aeg-deoxoartemisinin-*t*Bu oligomers (**136**, **140**, **145**, **147**) by using standard coupling protocol.

4.3.1 Synthesis of Fmoc-lys(Boc)-aeg-deoxoartemisinin-*t*Bu monomer (141)

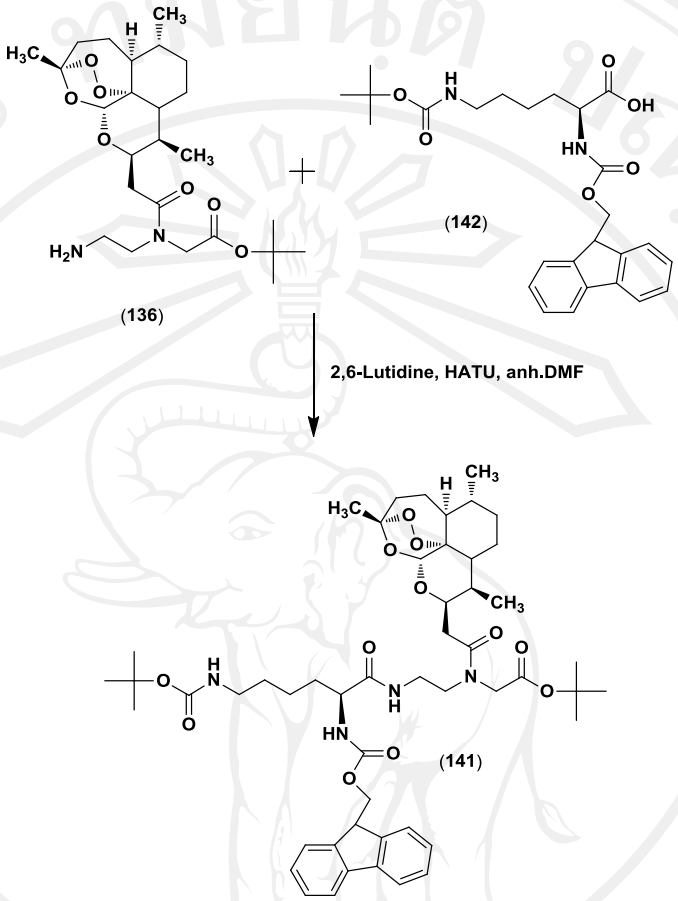

Scheme 4.10 Synthesis of Fmoc-lys(Boc)-aeg-deoxoartemisinin-*t*Bu monomer. (**141**)

To explore the effect of lysine to the bioactivity of the artemisinin-PNA conjugated, Fmoc-lys(Boc)-aeg-deoxoartemisinin-*t*Bu oligomers were synthesized. Coupling of NH_2-aeg-deoxoartemisinin-*t*Bu monomer (**136**) to Fmoc-lys(Boc)-OH (**142**) using HATU as coupling agent gave Fmoc-lys(Boc)-aeg-deoxoartemisinin-*t*Bu monomer (**141**) (70%) (Scheme 10). Further purification of Fmoc-lys(Boc)-aeg-deoxoartemisinin-*t*Bu monomer was performed by RP-HPLC using a C18 column running a gradient of acetonitrile. Major peak was collected and analysed by MS. ESI mass spectrometry showed molecular ion peak at 955.5049 correspond to $[M+Na]^+$ (Appendix II). The ^{1}H-NMR spectrum of this compound indicated the presence of

two rotamers (1 : 1 ratio) : 5.39 (1/2H, s, rotamer, H-12), 5.35 (1/2H, s, rotamer, H-12), 4.81 (1/2H, m, rotamer, H-10), 4.69 (1/2H, m, rotamer, H-10), 4.24 (1/2H, m, rotamer, H-16), 4.19 (1/2H, m, rotamer, H-16), 3.85 (1/2H, m, rotamer, H-16), 3.58 (1/2H, m, rotamer, H-16), 4.18-4.12 (1/2H, m, rotamer, H-19), 3.75-3.70 (1/2H, m, rotamer, H-19), 3.65 (1/2H, m, rotamer, H-19), 3.50 (1/2H, m, rotamer, H-19) (Appendix IV). The compound showed IR absorption at 3419 (υ_{N-H}, amide), 2930 (υ_{C-H}, alkane), 2870 (υ_{C-H}, alkane), 1714 ($\upsilon_{C=O}$, ester), 1655 ($\upsilon_{C=O}$, amide), 1509 ($\upsilon_{C=C}$, aromatic), 1450 ($\upsilon_{C=C}$, aromatic), 1366 (υ_{CH3}, alkane), 1232 ($\upsilon_{C-C(O)-C}$, ester), 1154, 1053 ($\delta_{=C-H}$, aromatic), 1040 ($\delta_{=C-H}$, aromatic), 876 (O-O) and 743 (δ_{C-H}, aromatic) cm^{-1} (Appendix III).

4.3.1.1 Synthesis of Fmoc-lys-aeg-deoxoartemisinin-*t*Bu monomer (148)

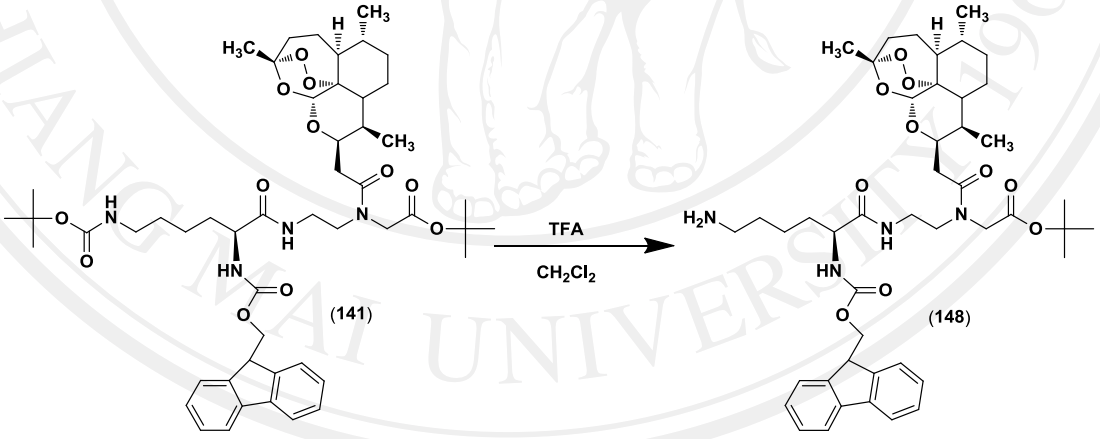

Scheme 4.11 Synthesis of Fmoc-lys-aeg-deoxoartemisinin-*t*Bu monomer. (**148**)

Fmoc-lys-aeg-deoxoartemisinin-*t*Bu monomer (**148**) was prepared by selectively deprotection of *t*-Boc at N terminal using TFA/CH_2Cl_2 of Fmoc-lys(Boc)-aeg-deoxoartemisinin-*t*Bu monomer (**141**) (Scheme 4.11). After the completion, the crude product was purified by flash chromatography using silica gel to afford the desired product **148** in moderate yields (62%). The purification of Fmoc-lys-aeg-

deoxoartemisinin-*t*Bu monomer was performed by RP-HPLC using a C18 column running a gradient of acetonitrile. Major peak was collected and analysed by MS. ESI mass spectrometry showed molecular ion peak at 833.4696 correspond to $[M+H]^+$ (Appendix II). In addition, the compound showed IR absorption at 3421 (υ_{N-H}, amide), 3063 ($\upsilon_{=C-H}$, aromatic), 2926 ($\upsilon_{C-H,}$ alkane), 2856 ($\upsilon_{C-H,}$ alkane), 1723 ($\upsilon_{C=O}$, ester), 1660 ($\upsilon_{C=O}$, amide), 1521 ($\upsilon_{C=C}$, aromatic), 1450 ($\upsilon_{C=C}$, aromatic), 1367 (υ_{CH3}, alkane), 1202 ($\upsilon_{C-C(O)-C}$, ester), 1152, 1043 (δ_{C-N}, amine), 883 (O-O) and 743 (δ_{C-H}, aromatic) cm^{-1} (Appendix III).

4.3.1.2 Synthesis of lys-aeg-deoxoartemisinin-*t*Bu monomer (152)

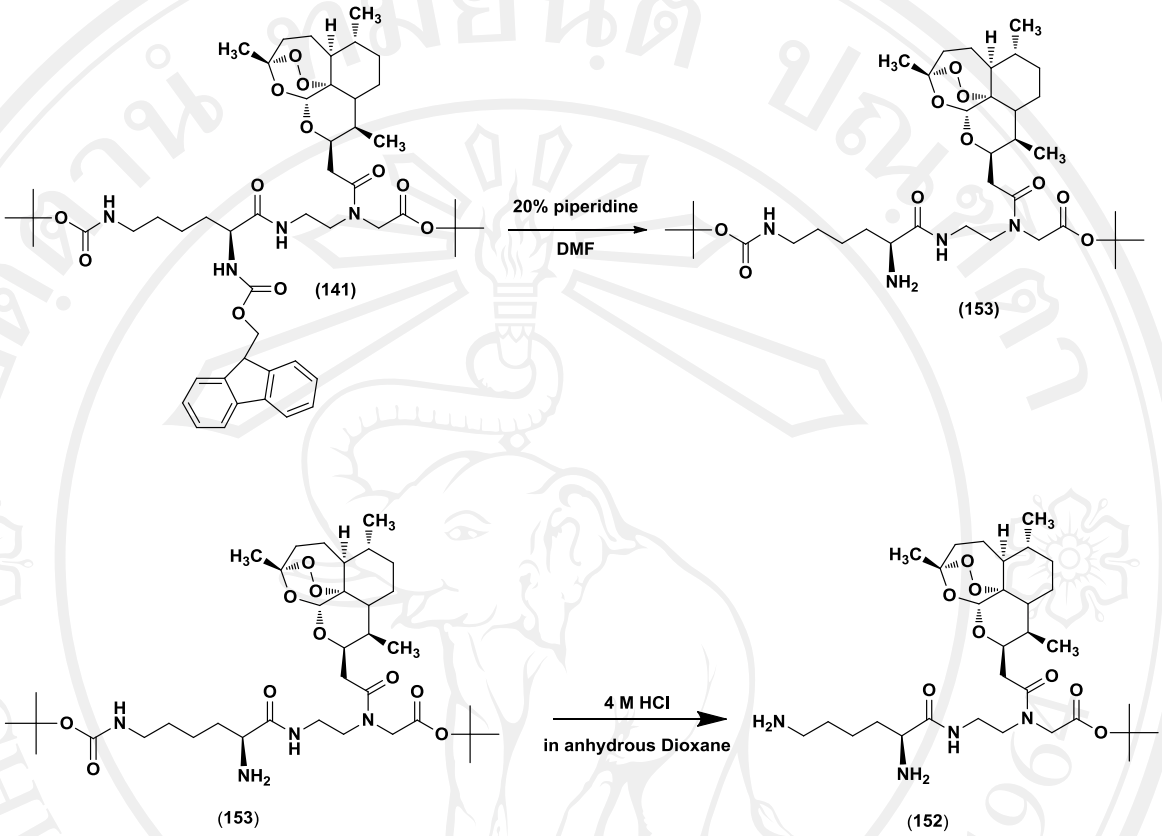

Scheme 4.12 Synthesis of lys-aeg-deoxoartemisinin-*t*Bu monomer. (**152**)

Deprotection of Fmoc was accomplished by treatment of Fmoc-lys(Boc)-aeg-deoxoartemisinin-*t*Bu monomer (**141**) with 20% piperidine in DMF. After purification by flash column chromatography, lys(Boc)-aeg-deoxoartemisinin-*t*Bu monomer (**153**) was obtained in excellent yields (94%). Subsequence removing the N-terminal Boc-protecting group was successfully processed by treatment with 4 M HCl in dioxane to give monomer **152** in quantitative yield (Scheme 4.12). ESI mass spectrometry showed molecular ion peak at 611.4014 correspond to $[M+H]^+$ (Appendix II). The compounds showed IR absorption at 3440 (υ_{N-H}, amide), 2959 (υC-H, alkane), 2917 (υC-H, alkane), 1644 (υC=O, amide), 1634 (δ_{N-H}, amide), 1462 (υ_{C-N}, amide), 1377

(υ_{CH3}, alkane), 1260 ($\upsilon_{C\text{-}C(O)\text{-}C}$, ester), 1157 ($\upsilon_{C\text{-}N}$, amine) and 718 ($\delta_{N\text{-}Hoop}$, amine) cm^{-1} (Appendix III).

4.3.2 Synthesis of Fmoc-lys(Boc)-aeg-deoxoartemisinin-*t*Bu dimer (143)

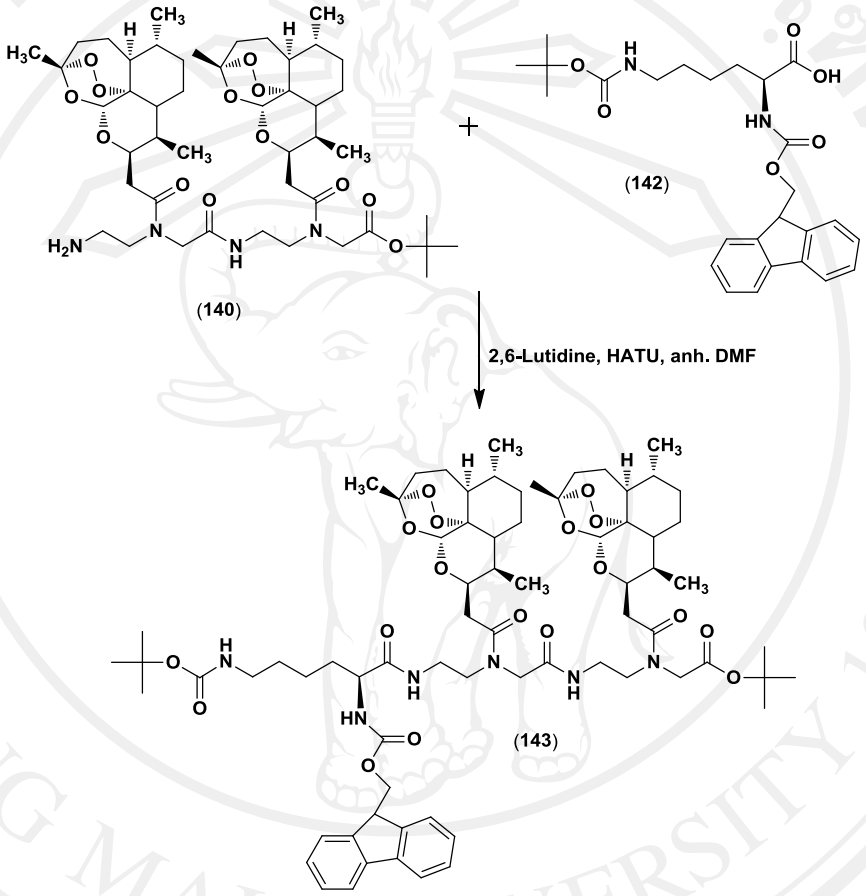

Scheme 4.13 Synthesis of Fmoc-lys(Boc)-aeg-deoxoartemisinin-*t*Bu dimer. (**143**)

To explore the effect of lysine to the bioactivity of the artemisinin-PNA dimer, Fmoc-lys(Boc)-aeg-deoxoartemisinin-*t*Bu dimers (**143**) was synthesized by the same strategy as Fmoc-lys(Boc)-aeg-deoxoartemisinin-*t*Bu monomer (**141**) Hence, Fmoc-aeg-deoxoartemisinin-*t*Bu dimer (**134**) was added 20% piperidine in DMF to obtain NH_2-aeg-deoxoartemisinin-*t*Bu dimer (**140**). Coupling of N-terminus of amine compound **140** Fmoc-lys(Boc)-OH **142** was performed by using HATU as coupling agent in the presence of 2,6-lutidine in DMF (Scheme 4.13). The coupling reaction

went smoothly to obtain the desired product **143** in approximately 50% yield after purification using flash column chromatography on silica gel. ESI mass spectrometry showed molecular ion peak at 1363.8578 correspond to $[M+Na]^+$ (Appendix II). In addition, the compound showed IR absorption at 3354 (υ_{N-H}, amide), 3063 ($\upsilon_{=C-H}$, aromatic), 2928 (υ_{C-H}, alkane), 1715 ($\upsilon_{C=O}$), 1659 ($\upsilon_{C=O}$, amide), 1525 ($\upsilon_{C=C}$, aromatic), 1452 ($\upsilon_{C=C}$, aromatic), 1366 (υ_{CH3}, alkane), 1248 ($\upsilon_{C-C(O)-C}$, ester), 1157, 1044 ($\delta_{=C-H}$, aromatic), 886 (O-O) and 739 (δ_{C-H}, aromatic) cm^{-1} (Appendix III).

4.3.2.1 Synthesis of Fmoc-lys-aeg-deoxoartemisinin-*t*Bu dimer (149)

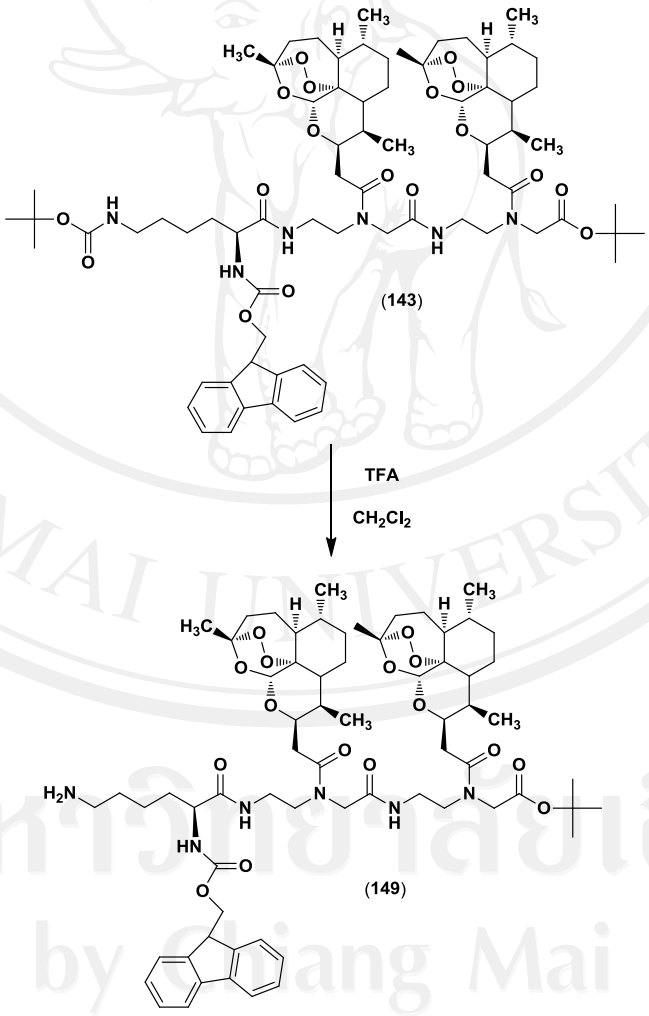

Scheme 4.14 Synthesis of Fmoc-lys-aeg-deoxoartemisinin-*t*Bu dimer. (**149**)

Fmoc-lys-aeg-deoxoartemisinin-*t*Bu dimer (**149**) was prepared by selectively deprotection of *t*-Boc at N terminal using TFA/CH_2Cl_2 (Scheme 4.14). After the completion, the crude product was purified by flash chromatography using silica gel to afford the desired product **149** in moderate yield (73%). The purification of Fmoc-lys-aeg-deoxoartemisinin-*t*Bu dimer was performed by RP-HPLC using a C18 column running a gradient of acetonitrile. Major peak was collected and analysed by MS. ESI mass spectrometry showed molecular ion peak at 1241.6925 correspond to $[M+H]^+$ (Appendix II). In addition, the compound showed IR absorption at 3391 (υ_{N-H}, amide), 3063 ($\upsilon_{=C-H}$, aromatic), 2949 (υ_{C-H}, alkane), 1719 ($\upsilon_{C=O}$, amide), 1651 ($\upsilon_{C=O}$, amide), 1536 ($\upsilon_{C=C}$, aromatic), 1451 ($\upsilon_{C=C}$, aromatic), 1371 (υ_{CH3}, alkane), 1213 ($\upsilon_{C-C(O)-C}$, ester), 1156, 1050 (δ_{C-N}, amine), 884 (O-O) and 735 (δ_{C-H}, aromatic) cm^{-1} (Appendix III).

4.3.2.2 Synthesis of lys-aeg-deoxoartemisinin-*t*Bu dimer (154)

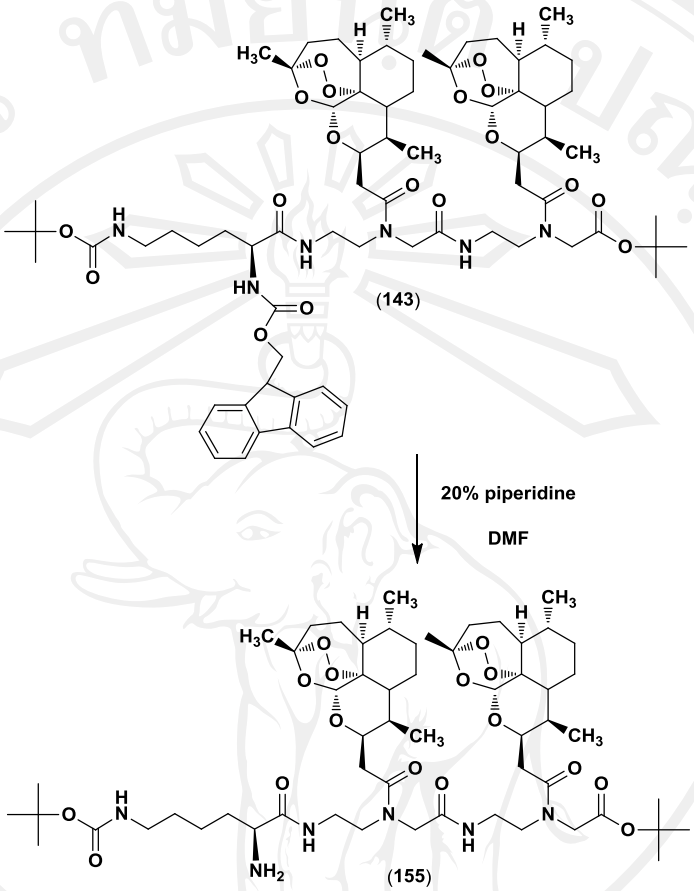

Scheme 4.15 Synthesis of lys-aeg-deoxoartemisinin-*t*Bu dimer. (**154**)

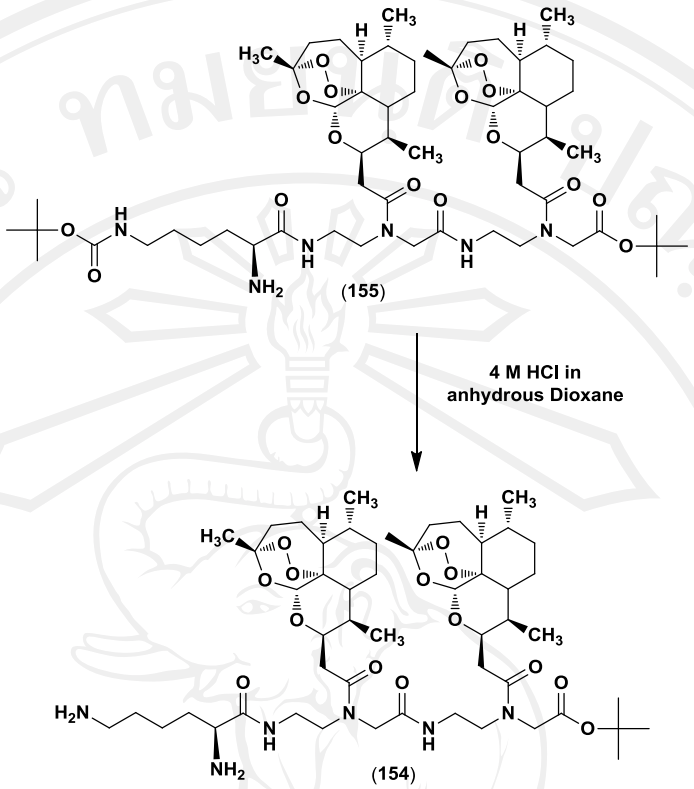

Scheme 4.15 (continued) Synthesis of lys-aeg-deoxoartemisinin-*t*Bu dimer. (**154**)

Deprotection of Fmoc is accomplished by treatment of Fmoc-lys(Boc)-aeg-deoxoartemisinin-*t*Bu dimer (**143**) with 20% piperidine in DMF. After purification by flash column chromatography, lys(Boc)-aeg-deoxoartemisinin-*t*Bu dimer (**155**) was obtained in moderate yields (66%). Subsequence removing the N-terminal Boc-protecting group was successfully processed by using 4 M HCl in dioxane to give dimer **154** in excellent yields (92%) (Scheme 4.15). ESI mass spectrometry showed molecular ion peak at 1019.6275 correspond to $[M+H]^+$ (Appendix II). In addition, the compound showed IR absorption at 3419 (υ_{N-H}, amide), 2926 (υ_{C-H}, alkane), 1634 ($\upsilon_{C=O}$, amide), 1539 (δ_{N-H}, amide), 1387 (υ_{CH3}, alkane), 1213 ($\upsilon_{C-C(O)-C}$, ester), 1157 (υ_{C-N}, amine), 964, 886 (O-O) and 734 (δ_{N-Hoop}, amine) (Appendix III).

4.3.3 Synthesis of Fmoc-lys(Boc)-aeg-deoxoartemisinin-*t*Bu trimer (144)

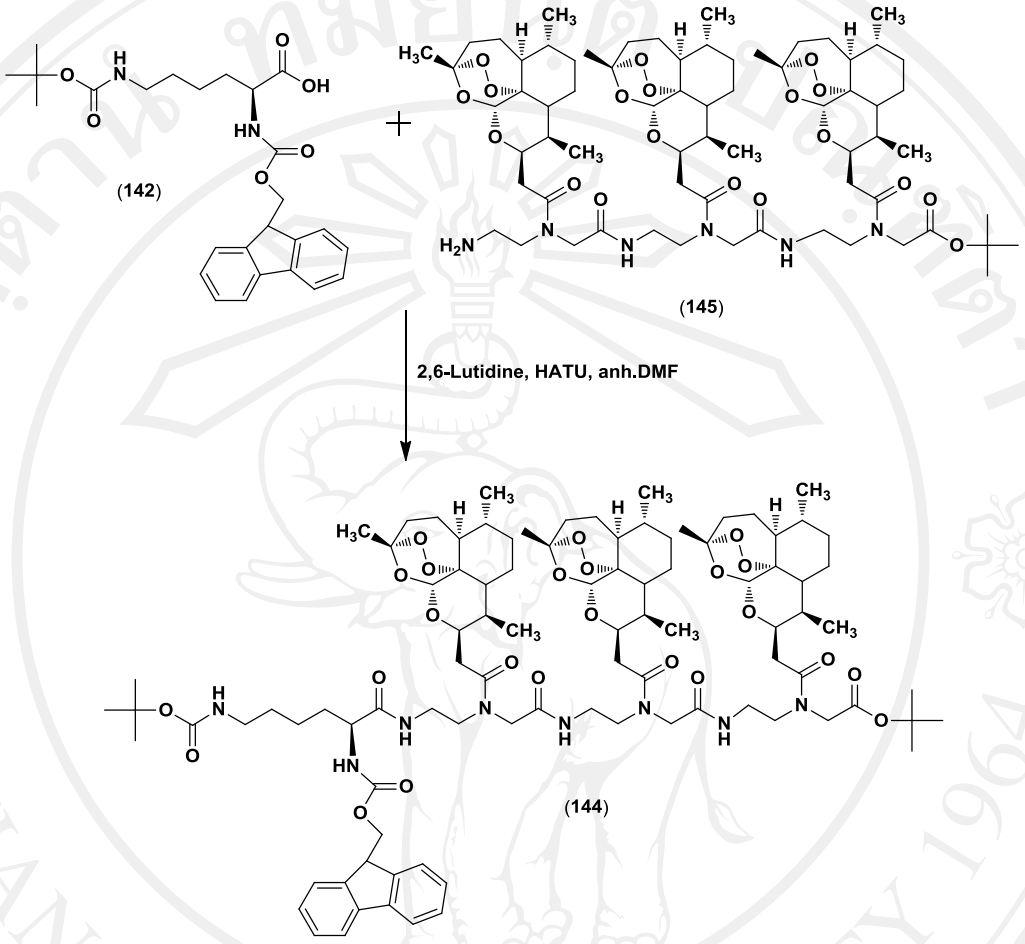

Scheme 4.16 Synthesis of Fmoc-lys(Boc)-aeg-deoxoartemisinin-*t*Bu trimer. (**144**)

Fmoc-lys(Boc)-aeg-deoxoartemisinin-*t*Bu trimer (**144**) was synthesized by the same strategy as Fmoc-lys(Boc)-aeg-deoxoartemisinin-*t*Bu monomer (**141**). Fmoc-aeg-deoxoartemisinin-*t*Bu trimer (**137**) was treated 20% piperidine in DMF to obtain NH_2-aeg-deoxoartemisinin-*t*Bu trimer (**145**). Coupling of N-terminus of amine compound **145** with C-terminus of Fmoc-lys(Boc)-OH **142** was performed by using HATU as coupling agent in the presence of 2,6-lutidine in DMF (Scheme 4.16). The coupling reactions went smoothly to afford the desired product **144** in approximately 50% yield after purification using flash column chromatography on silica gel. ESI mass spectrometry showed molecular ion peak at 1750.040 correspond to $[M+H]^+$

(Appendix II). In addition, the compound showed IR absorption at 3378 (υ_{N-H}, amide), 3067 ($\upsilon_{=C-H}$, aromatic), 2926 (υ_{C-H}, alkane), 1716 ($\upsilon_{C=O}$, ester), 1656 ($\upsilon_{C=O}$, amide), 1529 ($\upsilon_{C=C}$, aromatic), 1453 ($\upsilon_{C=C}$, aromatic), 1386 (υ_{CH3}, alkane), 1211 ($\upsilon_{C-C(O)-C}$, ester), 964, 886 (O-O) and 740 (δ_{C-H}, aromatic) cm^{-1} (Appendix III).

4.3.3.1 Synthesis of Fmoc-lys-aeg-deoxoartemisinin-*t*Bu trimer (150)

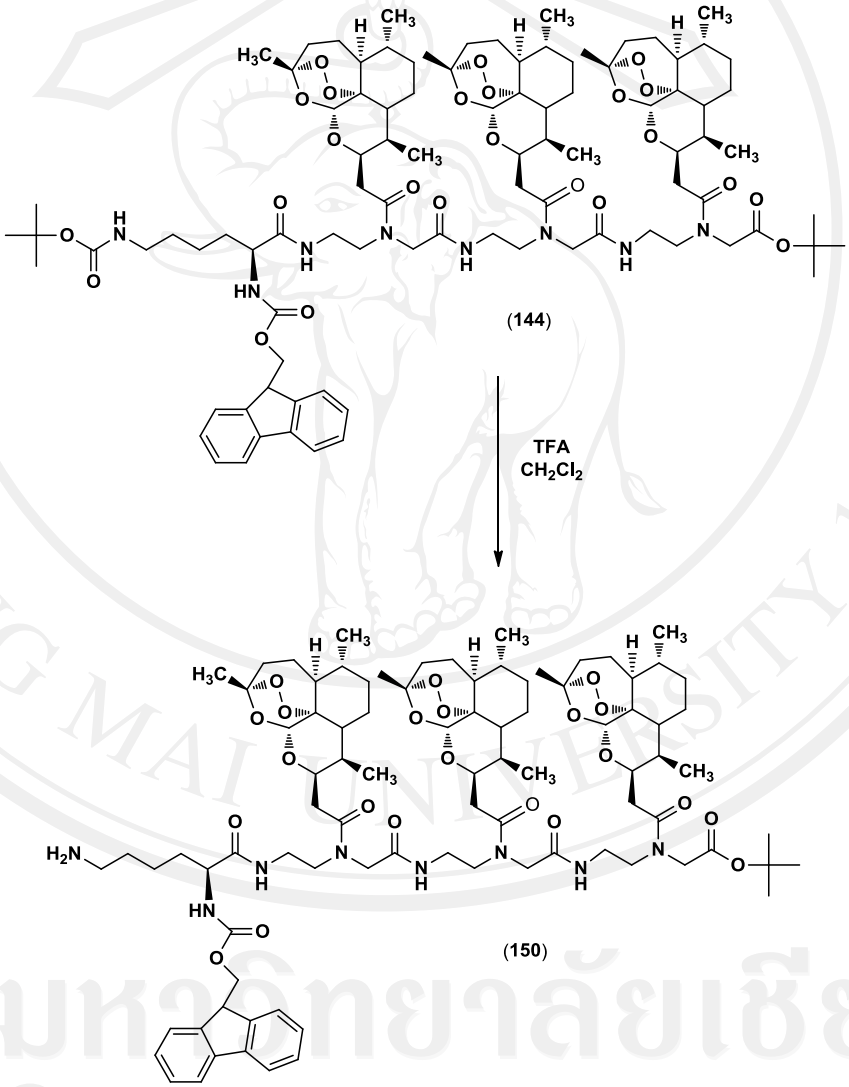

Scheme 4.17 Synthesis of Fmoc-lys-aeg-deoxoartemisinin-*t*Bu trimer. (**150**)

Fmoc-lys-aeg-deoxoartemisinin-*t*Bu trimer (**150**) was prepared by selectively deprotection of *t*-Boc at N-terminal using TFA/CH_2Cl_2 (Scheme 4.17). The completion of the reaction was monitored by TLC. The crude product was purified by flash chromatography using silica gel to afford the desired product **150** in low yields (29%). ESI mass spectrometry showed molecular ion peak at 1650.842 correspond to $[M+H]^+$ (Appendix II). This compound showed IR absorption at 3437 (υ_{N-H}, amide), 2924 (υ_{C-H}, alkane), 2852 (υ_{C-H}, alkane), 1644 ($\upsilon_{C=O}$, amide), 1541 ($\upsilon_{C=C}$, aromatic), 1455 ($\upsilon_{C=C}$, aromatic), 1384 (υ_{CH3}, alkane), 1210 ($\upsilon_{C-C(O)-C}$, ester), 1139, 1107, 1044 (δ_{C-N}, amine), 885 (O-O) and 741 (δ_{C-H}, aromatic) cm^{-1} (Appendix III).

4.3.4 Synthesis of Fmoc-lys(Boc)-aeg-deoxoartemisinin-*t*Bu tetramer (146)

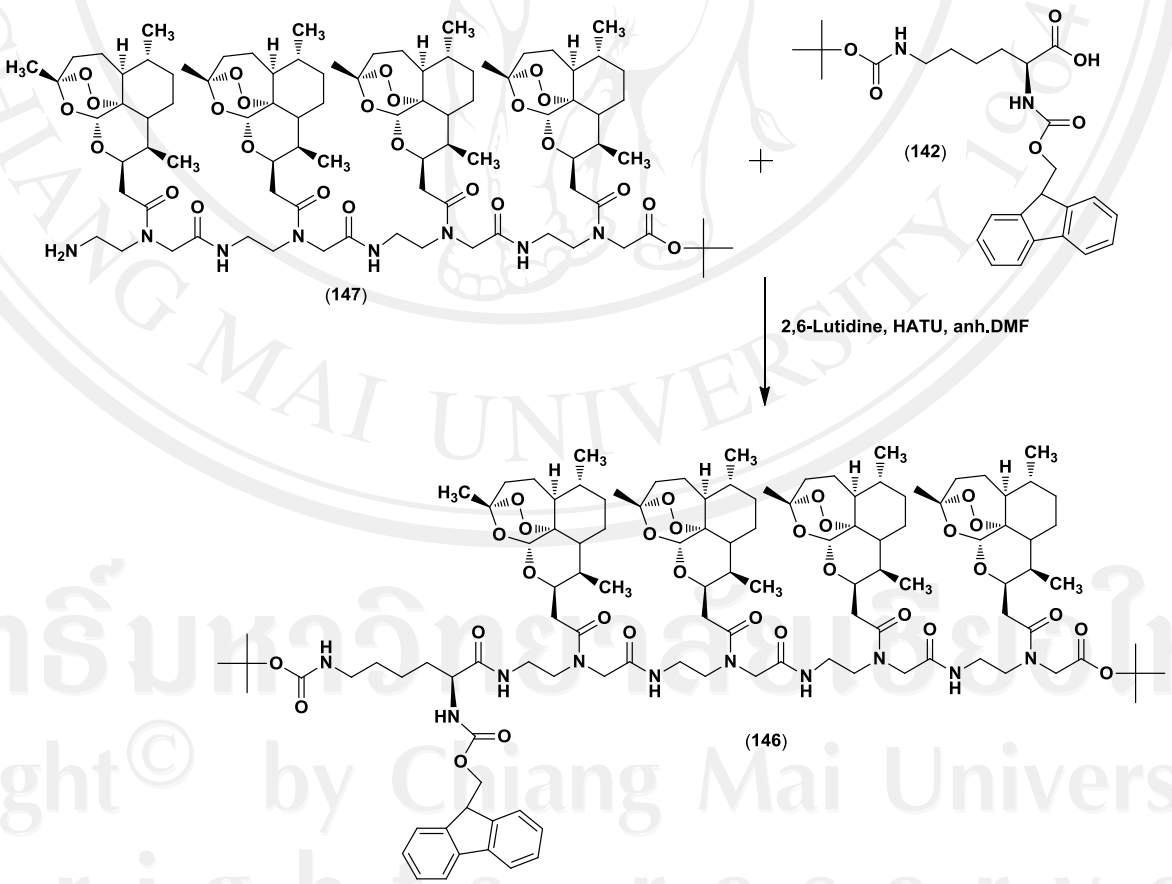

Scheme 4.18 Synthesis of Fmoc-lys(Boc)-aeg-deoxoartemisinin-*t*Bu tetramer. (**146**)

Fmoc-lys(Boc)-aeg-deoxoartemisinin-*t*Bu tetramers (**146**) was synthesized by the same strategy as Fmoc-lys(Boc)-aeg-deoxoartemisinin-*t*Bu monomer (**141**). Treatment of Fmoc-aeg-deoxoartemisinin-*t*Bu tetramer (**139**) using 20% piperidine in DMF obtained NH_2-aeg-deoxoartemisinin-*t*Bu tetramer (**147**). Coupling of N-terminus of amine compound **147** with C-terminus of Fmoc-lys(Boc)-OH **142** was performed by using HATU as coupling agent in the presence of 2,6-lutidine in DMF (Scheme 4.18). The coupling reactions went smoothly to afford the desired product **146** in approximately 65% yield after purification using flash column chromatography on silica gel. ESI mass spectrometry showed molecular ion peak at 2181.073 correspond to $[M+H]^+$ (Appendix II). In addition, the IR spectrum showed the absorptions at 3444 (υ_{N-H}, amide), 2925 (υ_{C-H}, alkane), 1651 ($\upsilon_{C=O}$, amide), 1644 (δ_{N-H}, amide), 1538 ($\upsilon_{C=C}$, aromatic), 1455 ($\upsilon_{C=C}$, aromatic), 1386 (υ_{CH3}, alkane), 1248 ($\upsilon_{C-C(O)-C}$, ester), 1171, 963, 886 (O-O) and 741 (δ_{C-H}, aromatic) cm^{-1} (Appendix III).

4.3.4.1 Synthesis of Fmoc-lys-aeg-deoxoartemisinin-*t*Bu tetramer (151)

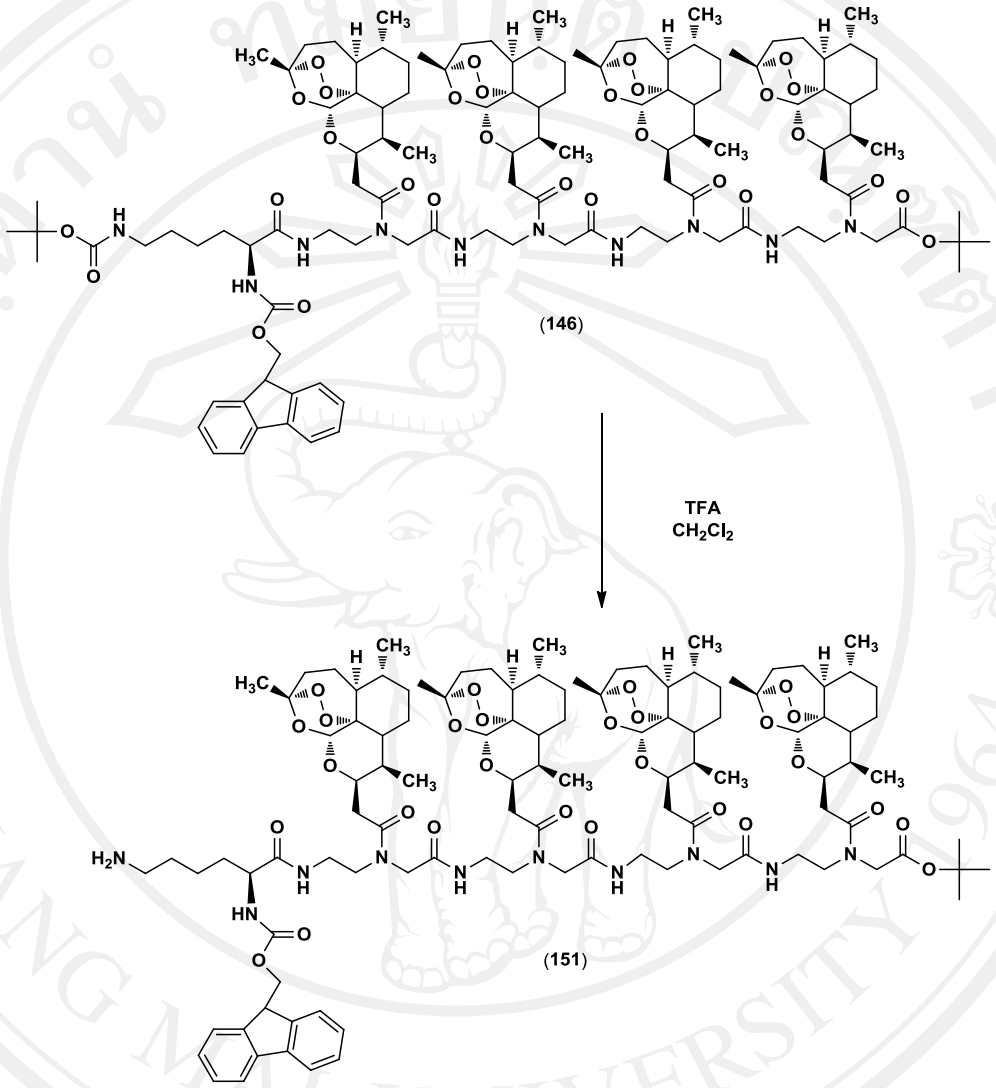

Scheme 4.19 Synthesis of Fmoc-lys-aeg-deoxoartemisinin-*t*Bu tetramer. (**151**)

Fmoc-lys-aeg-deoxoartemisinin-*t*Bu tetramer (**151**) was prepared by selectively deprotection of *t*-Boc at N-terminal using TFA/CH_2Cl_2 (Scheme 4.19). After the completion, the crude product was purified by flash chromatography using silica gel to afford the desired product **151** in low yields (23%). ESI mass spectrometry showed molecular ion peak at 2059.50 correspond to $[M+H]^+$ (Appendix II). This compound showed IR absorption at 3441 (υ_{N-H}, amide), 2926 (υ_{C-H}, alkane), 1644 ($\upsilon_{C=O}$, amide), 1634 (υ_{N-H}, amide), 1455 ($\upsilon_{C=C}$, aromatic), 1385 (υ_{CH3},

alkane), 1211 ($\upsilon_{C\text{-}C(O)\text{-}C}$, ester), 1171, 1138, 1081 ($\delta_{C\text{-}N}$, amine), 1003, 963, 886 (O-O) and 739 ($\delta_{C\text{-}H}$, aromatic) cm^{-1} (Appendix III).

4.4 Cyclization of NH_2-aeg-deoxoartemisinin-OH oligomers

To further investigate the possibility of cyclic conformation in improving the biological activities, cyclic oilgomers were prepared and investigated for their activities. Cyclic-aeg-deoxoartemisinin-oligomers were obtained by sequentially deprotection using TFA /CH_2Cl_2 and 20% piperidine in DMF followed by head-to-tail cyclization of the corresponding oligomers. The reaction proceeded smoothly to give the cyclic products in different yields and different reaction times upon the ring size.

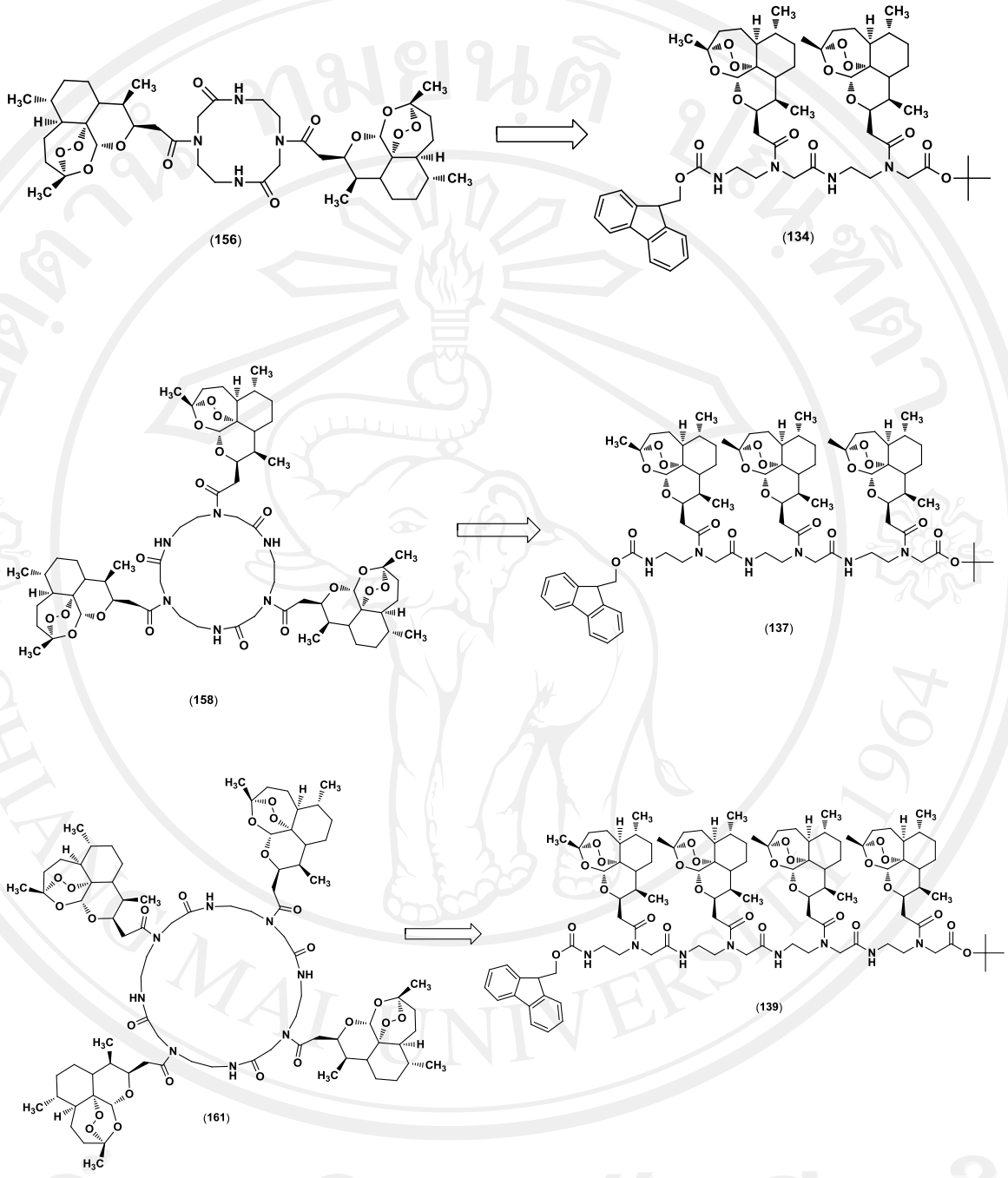

Scheme 4.20 Retrosynthesis of cyclic-aeg-deoxoartemisinin-oligomers.

4.4.1 Cyclization of NH_2-aeg-deoxoartemisinin-OH dimer (156)

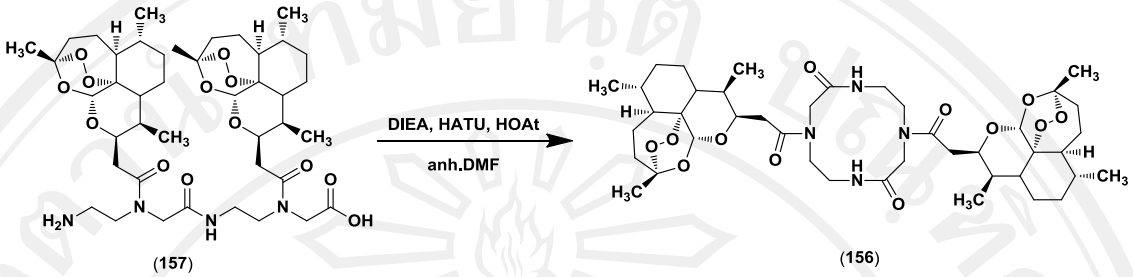

Scheme 4.21 Synthesis of cyclic-aeg-deoxoartemisinin-dimer. (**156**)

In order to synthesis of cyclic-aeg-deoxoartemisinin-dimer (**156**) (Scheme 4.21), dimer **134** was sequentially deprotection using TFA/CH_2Cl_2 and 20% piperidine in DMF to give **157** followed by cyclization under high dilution condition using HATU and HOAt as coupling agent to achieve the desired product **156** in low yields (42%) after purification by flash column chromatography. The further purification of cyclic-aeg-deoxoartemisinin-dimer **156** was performed by RP-HPLC using a C18 column running a gradient of acetonitrile. Major peak was collected and analysed by MS. ESI mass spectrometry showed molecular ion peak at 817.4593 correspond to $[M+H]^+$ (Appendix II). This compound showed IR absorption at 3413 (υ_{N-H}, amide), 2927 (υ_{C-H}, alkane), 1719 ($\upsilon_{C=O}$, ester), 1645 (C=O, amide), 1541 (δ_{N-H}, amide), 1459 (υ_{C-N}, amide), 1382 (υ_{CH3}, alkane) and 888 (O-O) cm^{-1} (Appendix III).

4.4.2 Cyclization of NH_2-aeg-deoxoartemisinin-OH trimer (158)

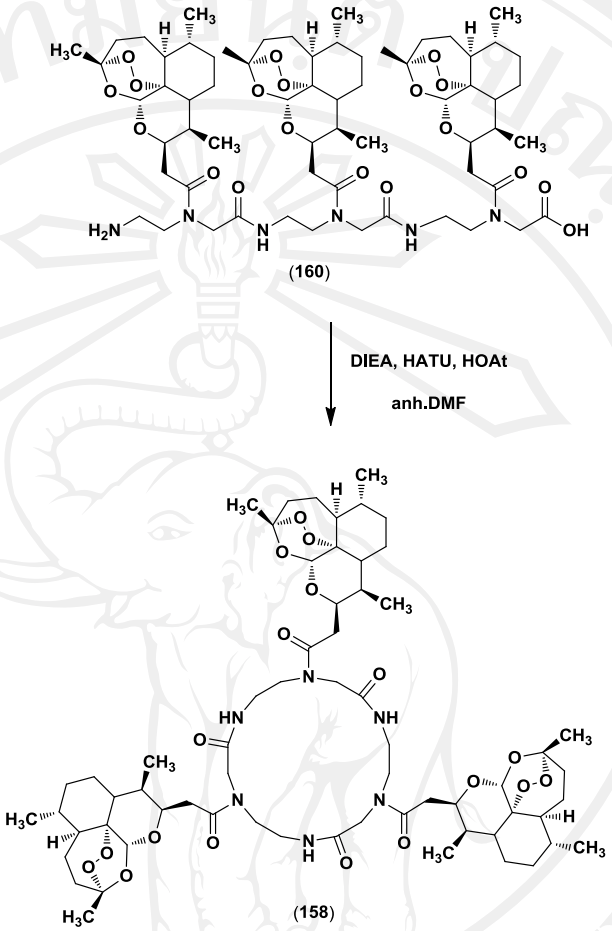

Scheme 4.22 Synthesis of cyclic-aeg-deoxoartemisinin-trimer. (**158**)

The cyclic-aeg-deoxoartemisinin-trimer (**158**) (Scheme 4.22) was synthesized from trimer **137**. Sequentially deprotection of trimer **137** by using TFA/CH_2Cl_2 and 20% piperidine in DMF to give **160** followed by cyclization under high dilution condition using HATU and HOAt as coupling agent to achieve the desired product **158** in low yields (33%) after purification by flash column chromatography. ESI mass spectrometry showed molecular ion peak at 1225.76 correspond to $[M+H]^+$ (Appendix II).

4.4.3 Cyclization of NH_2-aeg-deoxoartemisinin-OH tetramer (161)

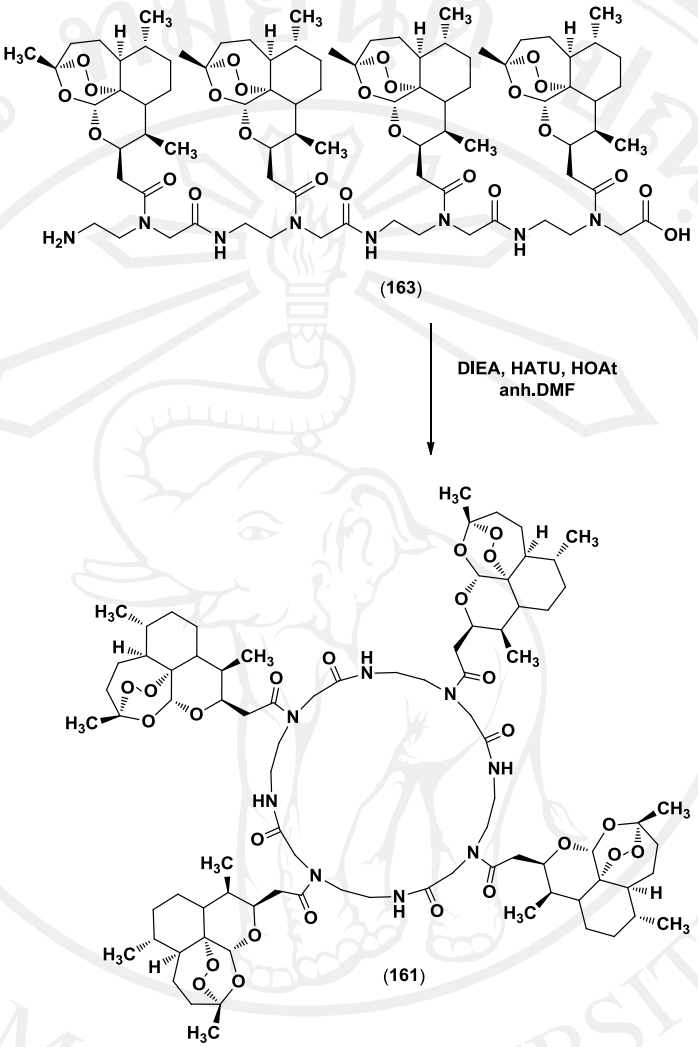

Scheme 4.23 Synthesis of cyclic-aeg-deoxoartemisinin-tetramer. (**161**)

In order to synthesis of cyclic-aeg-deoxoartemisinin-tetramer (**161**) (Scheme 4.23), tetramer **139** was sequentially deprotection using TFA/CH_2Cl_2 and 20% piperidine in DMF to give **163** followed by cyclization under high dilution condition using HATU and HOAt as coupling agent to give the desired cyclic tetramer **161** in fair yields (51%) after purification by flash column chromatography. ESI mass spectrometry showed molecular ion peak at 1633.89 correspond to $[M+H]^+$ (Appendix II).

4.5 Antimalarial Assessment of new deoxoartemisinin derivatives

All the synthetic derivatives prepared in this study have been evaluated for *in vitro* antimalarial activity against the chloroquine-resistance K1 strain of *P. falciparum* using artemisinin as positive control. The results are illustrated in Table 4.1. The results showed that all compounds were active against the chloroquine-resistance K1 strain of *P. falciparum*. On the contrary to our expectation, the most synthesized compounds (**134**, **137**, **139**, **141**, **143**, **148**, **149** and **156**) were less effective against *P.falciparum* than artemisinin and dihydroartemisinin with the exception of Fmoc-aeg-deoxoartemisinin-*t*Bu monomer (**132**). The monomer **132** is the most active compound with IC_{50} 4.46 nM and is two times greater than artemisinin (**9**). Moreover, Fmoc-lys(Boc)-aeg-deoxoartemisinin-*t*Bu monomer (**141**) and Fmoc-lys-aeg-deoxoartemisinin-*t*Bu monomer (**148**) are much less active than artemisinin against the chloroquine-resistance K1 strain of *P. falciparum*. This indicated that adding amino acid moiety to the N-terminus of the peptide chain did not increase the antimalarial activity. The antimalarial activity of compound **141**, **148**, **143** and **149** were less active than artemisinin (**9**) (3 times, 34 times, 2 times and 33 times, respectively). The activity showed that Fmoc-aeg-deoxoartemisinin-*t*Bu monomer (**132**) is more active than Fmoc-aeg-deoxoartemisinin-*t*Bu dimer (**134**), Fmoc-aeg-deoxoartemisinin-*t*Bu trimer (**137**) and Fmoc-aeg-deoxoartemisinin-*t*Bu tetramer (**139**). In contrast with our expectation, the cyclic dimer (**156**) showed poorer activity than Fmoc-aeg-deoxoartemisinin-*t*Bu monomer (**132**) against the chloroquine-resistance K1 strain of *Plasmodium falciparum* with IC_{50} of 3.28 µM.

Table 4.1 *In vitro* antimalarial activity of all compounds against K1 strains of *P. falciparum*.

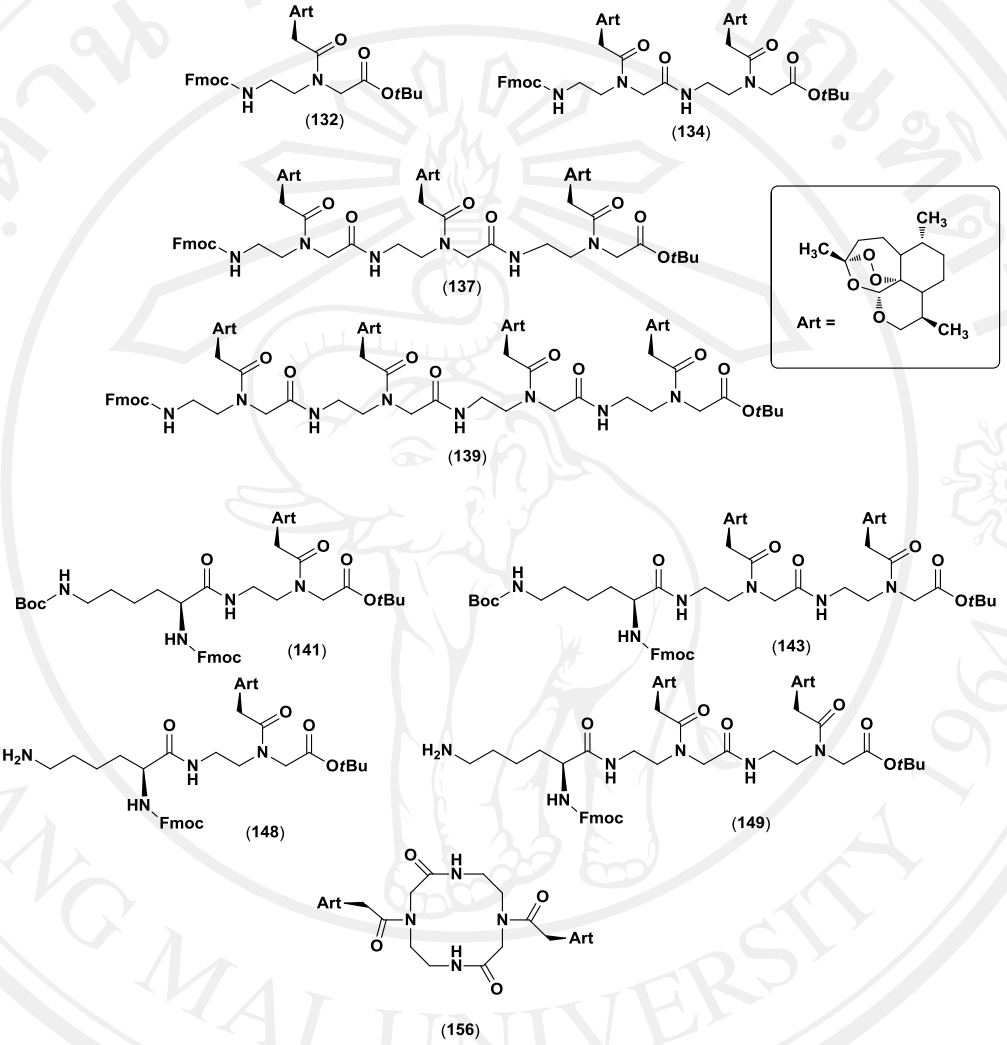

Compound	IC_{50}	Compound	IC_{50}
132	4.46	**134**	19.94
137	27.06	**139**	157.17
141	34.19	**143**	23.18
156	3280.37	**148**	336.13
149	330.20	Artemisinin (**9**)	9.98

Anticancer activities

In this study, *in-vitro* study was undertaken to demonstrate the effects of all synthesized oligomers on different classes of human cancer and normal cells. The purpose of the study was to determine the selective of the synthesized compounds against various cancer cells. MTT based cytotoxic assay was carried out using four cancerous cell lines, HT-29 (Human colonic adenocarcinoma cell line), Caco-2 (Human colonic adenocarcinoma cell line), A549 (Human lung adenocarcinoma epithelial cell line) and B16F10 (Mouse melanoma cell line) and normal cell line, L929 (Mouse, C34/An, connective tissue) and the results were shown in Table 4.2-4.6. The dihydroartemisinin (**23**) was used as a control. The IC_{50} values were calculated from the dose-response curves for the viability of cancer cell lines by using BioDataFit software v 1.02 from Chang Biosciences Inc. All compounds were tested for the toxicity against to normal cells to evaluate the candidates for anticancer drugs. The results are shown in Table 4.2.

Table 4.2 *In vitro* anticancer activity of deoxoartemisinin derivatives against L929 cell line.

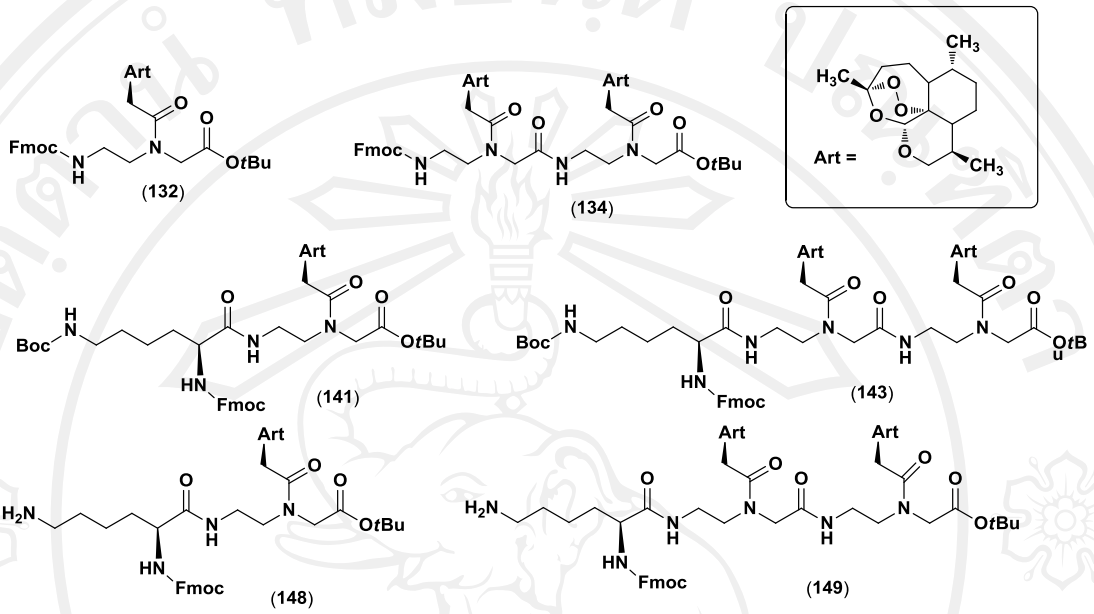

Compound	LD_{50}	Compound	LD_{50}
132	18.22 ± 0.18	**134**	9.77 ± 0.80
141	5.63 ± 0.52	**143**	4.55 ± 0.15
148	45.26 ± 0.30	**149**	38.13 ± 0.6

* LD_{50} = µM, DHA = 32.92 ± 0.47 µM

4.6.1 The cytotoxicity against normal cell line (L929)

Fmoc-aeg-deoxoartemisinin-*t*Bu monomer (**132**), Fmoc-lys(Boc)-aeg-deoxoartemisinin-*t*Bu monomer (**141**) and Fmoc-lys-aeg-deoxoartemisinin-*t*Bu monomer (**148**), Fmoc-aeg-deoxoartemisinin-*t*Bu dimer (**134**), Fmoc-lys(Boc)-aeg-deoxoartemisinin-*t*Bu dimer (**143**) and Fmoc-lys-aeg-deoxoartemisinin-*t*Bu dimer (**149**) were evaluated against normal cell line. The results were shown in Table 4.2.

The results showed that Fmoc-lys-aeg-deoxoartemisinin-*t*Bu monomer (**148**) has the lowest toxicity to normal tissue (LD_{50} = 45.26 µM), and lower toxicity than DHA (LD_{50} = 32.92 µM). On the contrary, Fmoc-lys(Boc)-aeg-deoxoartemisinin-*t*Bu dimer (**143**) has the highest toxicity to normal tissue (LD_{50} = 4.55 µM) and more toxic than dihydroartemisinin (LD_{50} = 32.92 µM) (Table 4.2 and Figure 4.1). Compounds **132, 134, 141, 143, 148** and **149** have cytotoxicity against normal cell in the range of 4.55-45.26 µM.

The fully protected form of monomer **132** showed less toxicity (LD_{50} = 18.22 µM) to than the corresponding dimer **134** (LD_{50} = 9.77 µM) while adding Boc-protected Lysine amino acid to the N-terminus of monomer **132** to give monomer lysine **141** caused higher toxicity (LD_{50} = 5.63 µM) than monomer **132** (LD_{50} = 18.22 µM). The same result with monomer, dimer lysine **143** exhibited two times more toxicity (LD_{50} = 4.55 µM) than dimer **134** (LD_{50} = 9.77 µM). This indicated that adding lysine Boc-protected Lys amino acid to the N-terminus of monomer **132** and dimer **134** can increase toxicity of the corresponding C-10 non-acetal derivatives.

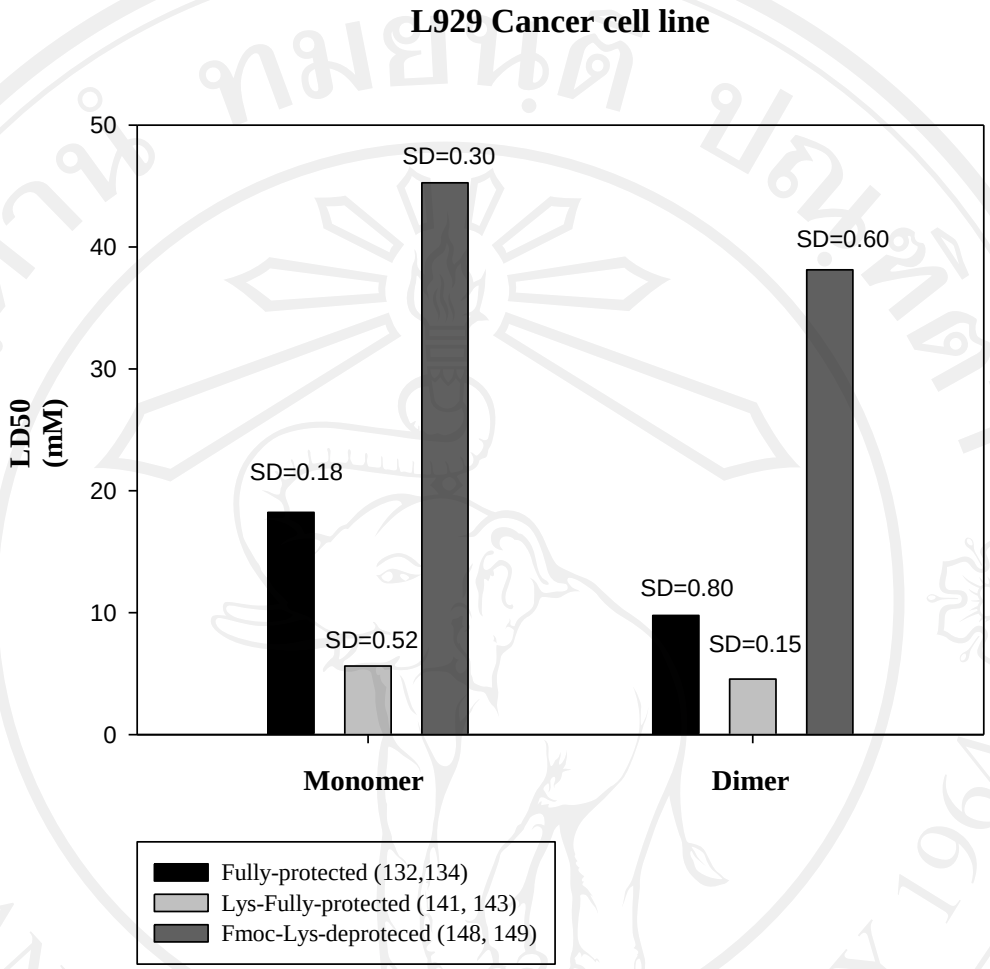

Figure 4.1 LD_{50} values of monomer (**132, 141, 148**) and dimer (**134, 143, 149**) compound against normal cancer cell : LD_{50} of DHA = 32.92 µM.

Furthermore, deprotection of Boc-lysine of monomer lysine **141** to afford amino monomer **148** exhibited less toxicity (LD_{50} = 45.26 µM) than monomer **132** (LD_{50} = 18.22 µM) and monomer lysine **141** (LD_{50} = 5.63 µM). The same results were received for amino dimer lysine (**149**). The deprotection of Boc-lysine of dimer lysine **143** to afford amino dimer **149** showed less toxic (LD_{50} = 38.50 µM) than the corresponding dimer **134** (LD_{50} = 9.77 µM) and dimer lysine **143** (LD_{50} = 4.55 µM).

Table 4.3 *In vitro* anticancer activity of deoxoartemisinin derivatives against HT-29 cell line.

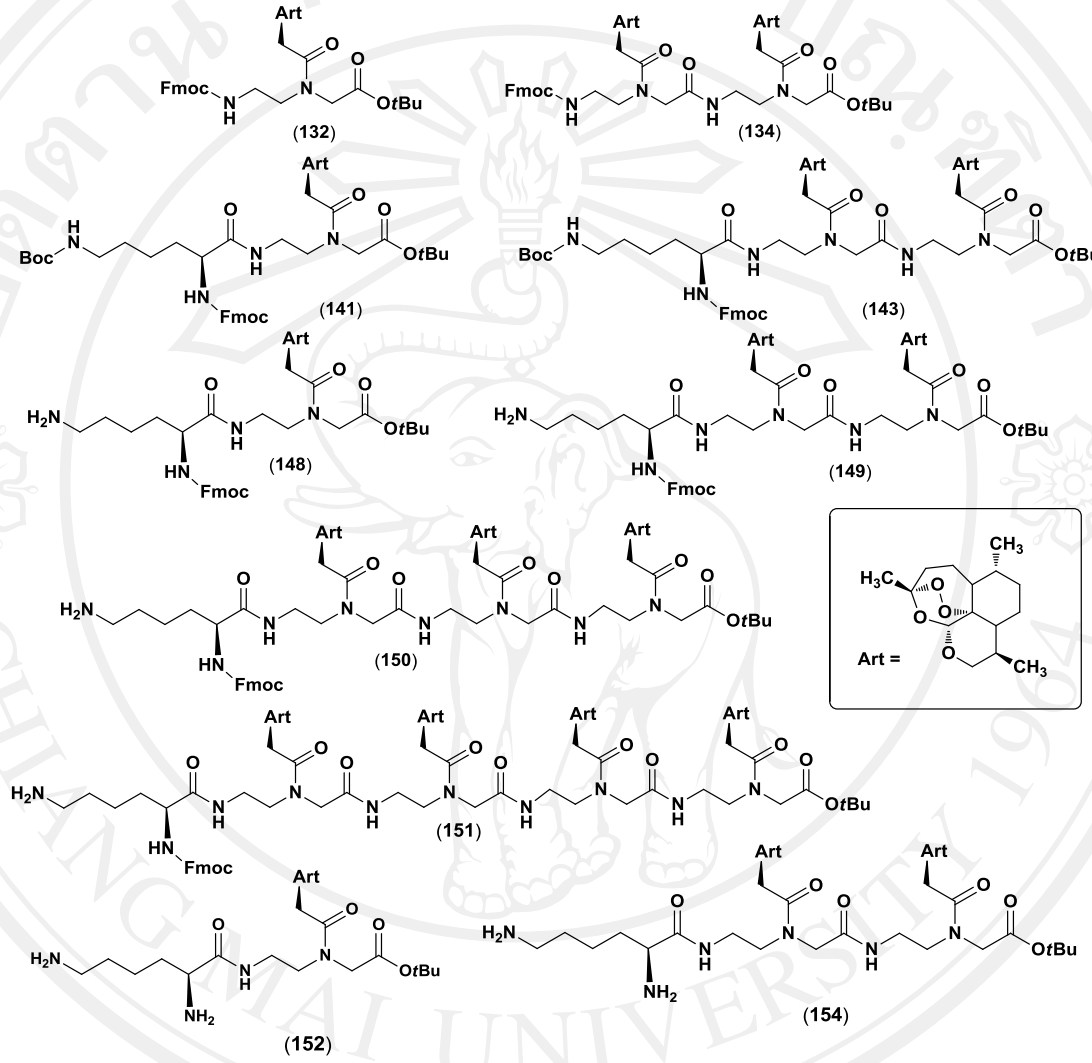

Compound	IC_{50}	Compound	IC_{50}
132	8.91 ± 0.22	**134**	5.36 ± 0.28
141	3.64 ± 0.24	**143**	4.36 ± 0.10
148	0.63 ± 0.22	**149**	0.18 ± 0.37
150	0.30 ± 0.40	**151**	0.45 ± 0.24
152	19.59 ± 0.17	**154**	11.08 ± 0.12

* IC_{50} = µM, DHA = 20.51 ± 0.28 µM

4.6.2 The cytotoxicity against colon cancer cell line (HT-29)

Fmoc-aeg-deoxoartemisinin-*t*Bu monomer (**132**), Fmoc-lys(Boc)-aeg-deoxoartemisinin-*t*Bu monomer (**141**), Fmoc-lys-aeg-deoxoartemisinin-*t*Bu monomer (**148**), lys-aeg-deoxoartemisinin-*t*Bu monomer (**152**), Fmoc-aeg-deoxoartemisinin-*t*Bu dimer (**134**), Fmoc-lys(Boc)-aeg-deoxodeoxoartemisinin-*t*Bu dimer (**143**), Fmoc-lys-aeg-deoxoartemisinin-*t*Bu dimer (**149**) and lys-aeg-deoxoartemisinin-*t*Bu dimer (**154**) were evaluated against HT-29 cell line. The results were shown in Table 4.3 and Figure 4.2.

The results showed that Fmoc-lys-aeg-deoxoartemisinin-*t*Bu dimer (**149**) was the most potent activity (IC_{50} = 0.18 µM) against HT-29 cell line and higher activity than DHA (IC_{50} = 20.59 µM). On the contrary, lys-aeg-deoxoartemisinin-*t*Bu monomer (**152**) exhibited the lowest activity against HT-29 cell line with IC_{50} of 19.59 µM. All compounds showed cytotoxicity against HT-29 cell line in the range of 0.18-19.59 µM.

All dimers were more potent than the correponding monomers. For example, fully protected dimer **134** showed two times higher activity (IC_{50} = 5.36 µM) than fully protected monomer **132** (IC_{50} = 8.91 µM), whereas amino dimer lysine **149** exhibited three times higher activity (IC_{50} = 0.18 µM) than amino monomer lysine **148** (IC_{50} = 0.63 µM). Adding Boc-protected Lys amino acid to the N-terminus of monomer **132** to give monomer lysine **141** which exhibited caused two times higher activity (IC_{50} = 3.64 µM) against HT-29 cell line than monomer **132** (IC_{50} = 8.91 µM) while dimer lysine **143** (IC_{50} = 4.36 µM) which obtained by adding Boc-protected Lys amino acid to the N-terminus of dimer **134** was comparable to the corresponding dimer **134** (IC_{50} = 5.36 µM).

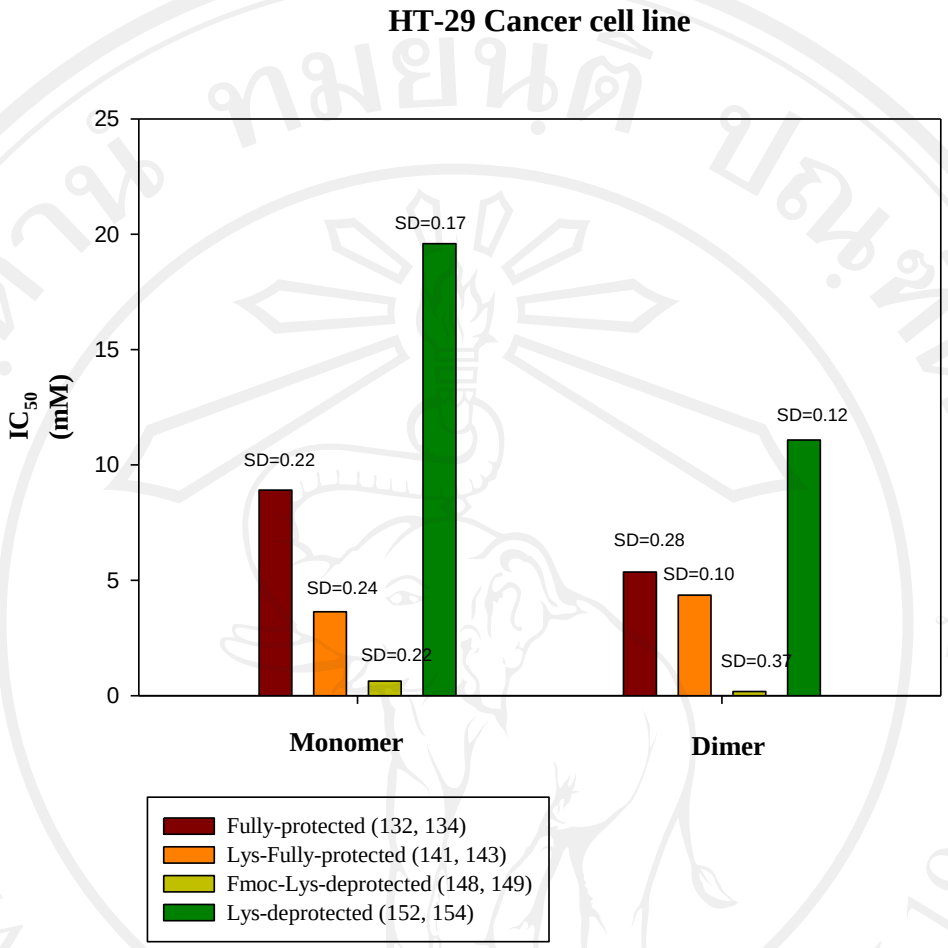

Figure 4.2 Comparison of the cytotoxicities of monomer (**132, 141, 148, 152**) and dimer (**134, 143, 149, 154**) tested on HT-29 cancer cell : IC_{50} of DHA = 20.59 µM.

On the other hand, deprotection of Boc-lysine amino acid of monomer lysine **141** to give amino monomer lysine **148** exhibited greater activity (IC_{50} = 0.63 µM) than fully protected monomer lysine **141** (IC_{50} = 3.64 µM). The same results for amino dimer lysine **149** were obtained as amino monomer lysine **148**. The activity of amino dimer lysine **149** showed 24 times higher activity (IC_{50} = 0.18 µM) than fully protected dimer lysine **143** (IC_{50} = 4.36 µM). The results suggested that introducing a lysine-based monomer into PNA oligomers can increase anticancer activity which are presumably due to hydrophilic group of compounds increase their aqueous

solubility.[84] In addition, the removal *t*Boc & Fmoc Lys protection group of monomer lysine **141** and dimer lysine **143** gave diamino monomer lysine **152** and diamino dimer lysine **154**. The results showed that the activity of diamino monomer lysine **152** (IC_{50} = 19.59 µM) was less active than amino monomer lysine **148** (IC_{50} = 0.63 µM). The same results for diamino dimer lysine **154** were obtained as diamino monomer lysine **152**. The activity of diamino dimer lysine **154** showed less activity (11.08 µM) than amino dimer lysine **149** (IC_{50} = 0.18 µM).

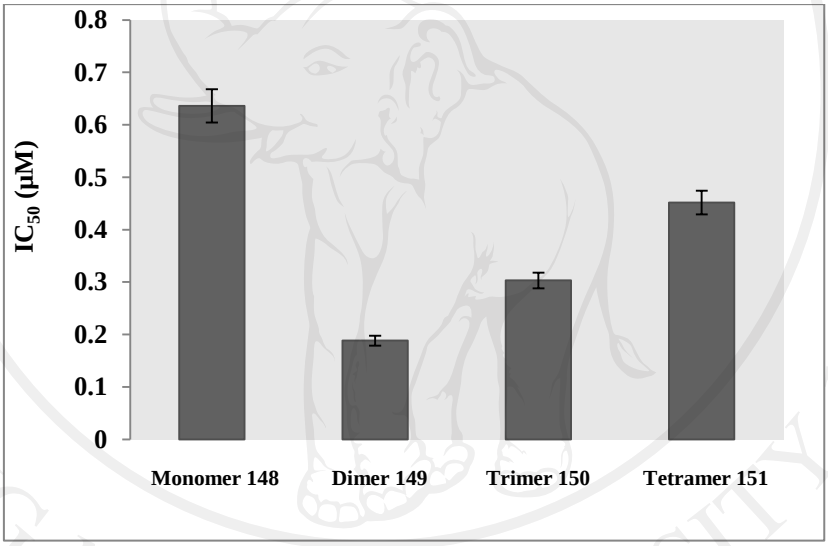

Figure 4.3 Comparison of the cytotoxicities of Fmoc-lys-aeg-deoxoartemisinin-*t*Bu oligomers tested on HT-29 cancer cell.

The activity of higher oligomers such as Fmoc-lys-aeg-deoxoartemisinin-*t*Bu trimer (**150**) and Fmoc-lys-aeg-deoxoartemisinin-*t*Bu tetramer (**151**) were evaluated and the results were shown in Table 4.3 and Figure 4.3. The results revealed that Fmoc-lys-aeg-deoxoartemisinin-*t*Bumonomer (**148**) is the least active compound with an IC_{50} 0.63 µM followed by Fmoc-lys-aeg-deoxoartemisinin-*t*Bu tetramer (**151**) (IC_{50} = 0.45 µM), Fmoc-lys-aeg-deoxoartemisinin-*t*Bu trimer (**150**) (IC_{50} = 0.30 µM) and Fmoc-lys-aeg-deoxoartemisinin-*t*Bu dimer (**149**) with IC_{50} of 0.18 µM. It was

observed that increasing of artemisinin-monomer unit did not increase the activity against HT-29 cell line which is presumably due to their low solubility.[103] However, the repeating unit of *N*-(2-aminoethyl) glycine (aeg) dimer, trimer and tetramer are more effective than dihydroartemisinin (IC_{50} = 20.59 μM).

Table 4.4 *In vitro* anticancer activity of deoxoartemisinin derivatives against Caco-2 cell line.

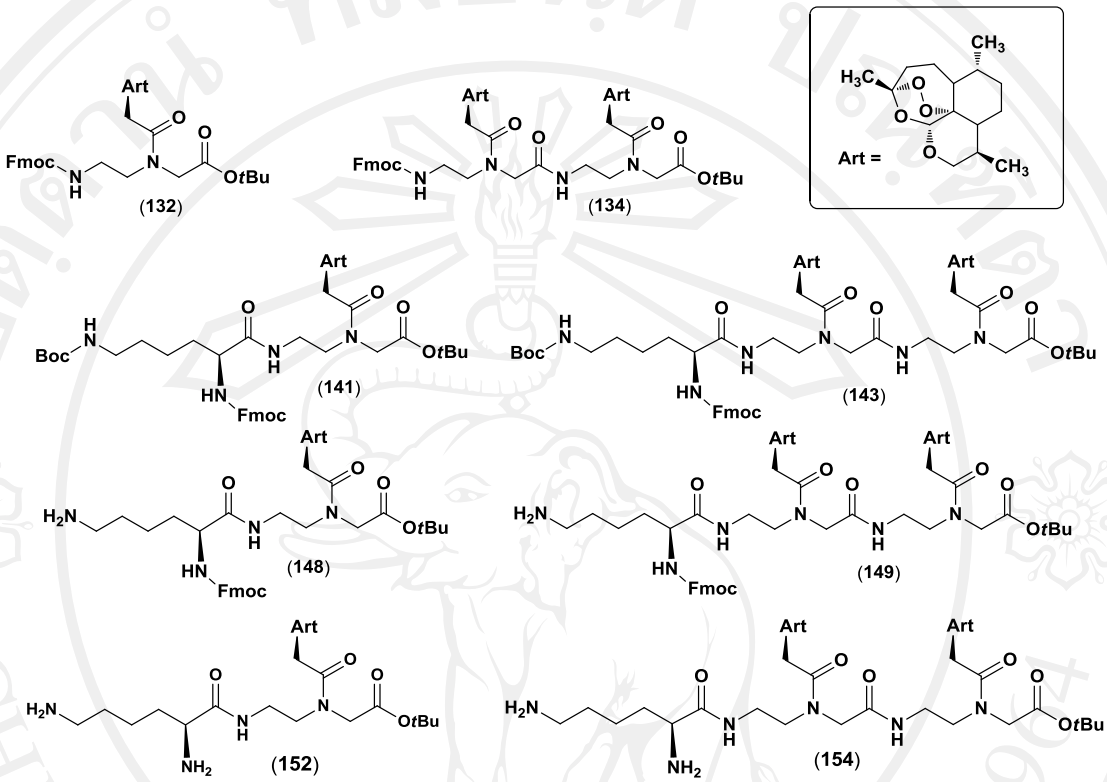

Compound	IC_{50}	Compound	IC_{50}
132	5.36 ± 0.20	**134**	2.87 ± 0.20
141	11.95 ± 0.24	**143**	8.03 ± 0.42
148	4.38 ± 0.17	**149**	2.04 ± 0.31
152	14.71 ± 0.14	**154**	3.58 ± 0.98

* IC_{50} = µM, DHA = 26.87 ± 0.11 µM

4.6.3 The cytotoxicity against colon cancer cell line (Caco-2)

Fmoc-aeg-deoxoartemisinin-*t*Bu monomer (**132**), Fmoc-lys(Boc)-aeg-deoxoartemisinin-*t*Bu monomer (**141**), Fmoc-lys-aeg-deoxoartemisinin-*t*Bu monomer (**148**), lys-aeg-deoxoartemisinin-*t*Bu monomer (**152**), Fmoc-aeg-deoxoartemisinin-*t*Bu dimer (**134**), Fmoc-lys(Boc)-aeg-deoxoartemisinin-*t*Bu dimer (**143**), Fmoc-lys-aeg-deoxodeoxoartemisinin-*t*Bu dimer (**149**) and lys-aeg-deoxoartemisinin-*t*Bu dimer (**154**) were evaluated against Caco-2 cell line. The results were shown in Table 4.4 and Figure 4.4.

All compounds have cytotoxicity against Caco-2 cell line in the range of 2.04-14.71 µM which are higher than DHA (IC_{50} = 26.87 µM). The same trend of activity against Caco-2 cancer cell line was obtained with both the monomer and dimer derivatives. It was indicated that the lysine unit has a marked influence on the activity against Caco-2 cell line of both monomer series and dimer series. The best activity against Caco-2 cell line was observed for Fmoc-lys-aeg-deoxoartemisinin-*t*Bu dimer (**149**). The dimer **149** showed the highest activity against Caco-2 cancer cell with IC_{50} of 2.04 µM followed by Fmoc-aeg-deoxoartemisinin-*t*Bu dimer (**134**), lys-aeg-deoxoartemisinin-*t*Bu monomer (**154**), Fmoc-lys-aeg-deoxoartemisinin-*t*Bu monomer (**148**), Fmoc-aeg-deoxoartemisinin-*t*Bu monomer (**132**), Fmoc-lys(Boc)-aeg-deoxoartemisinin-*t*Bu dimer (**143**) and Fmoc-lys(Boc)-aeg-deoxoartemisinin-*t*Bu monomer (**141**) with IC_{50} of 2.87 µM, 3.58 µM, 4.38 µM, 5.36 µM, 8.03 µM and 11.95 µM, respectively. Fully removing the amino protecting group of Fmoc-lys(Boc)-aeg-deoxoartemisinin-*t*Bu monomer (**141**) gave lys-aeg-deoxoartemisinin-*t*Bu monomer (**152**) which exhibited the lowest activity against Caco-2 cell line with IC_{50} of 14.71 µM.

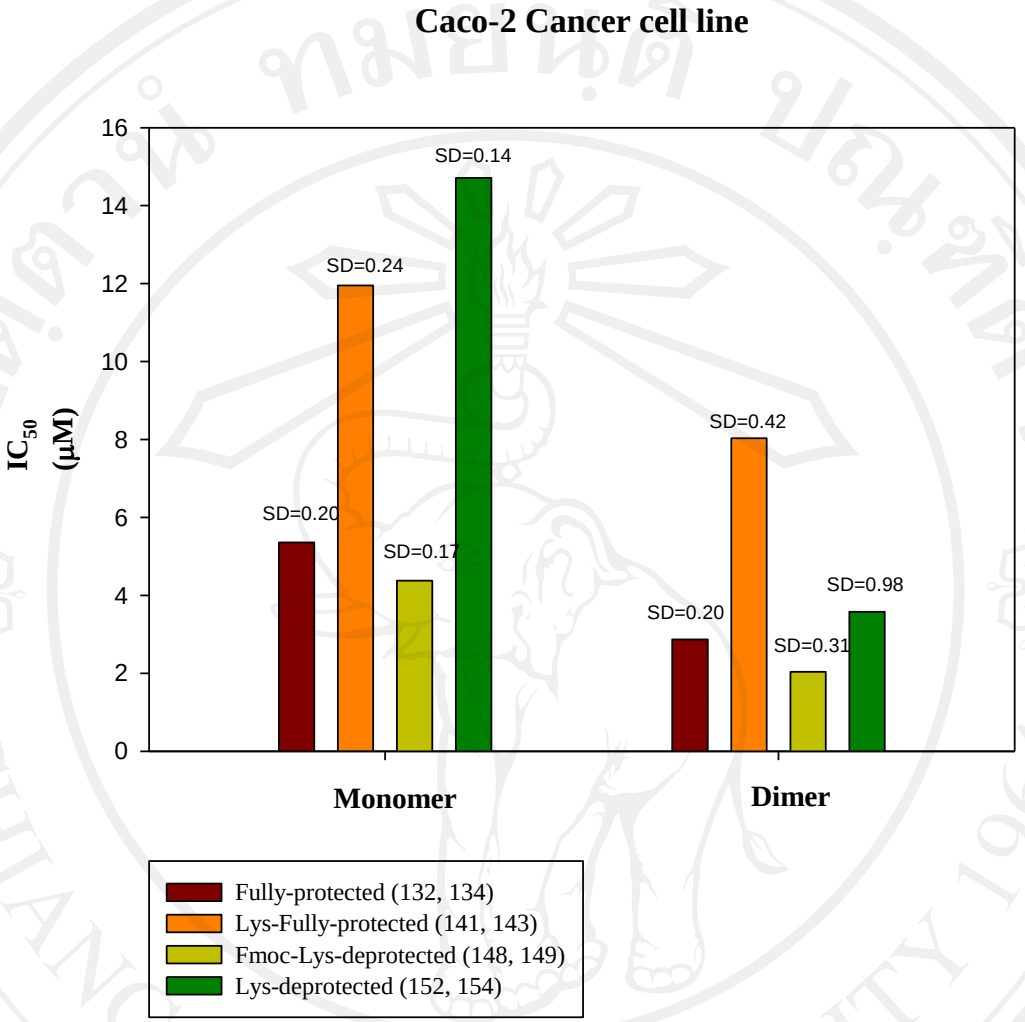

Figure 4.4 Comparison of the cytotoxicities of (**132, 141, 148, 152**) and dimer (**134, 143, 149, 154**) tested on Caco-2 cancer cell : IC_{50} of DHA = 26.87 µM.

All dimers were more potent than the correponding monomers. For example, fully protected dimer **134** showed two times higher activity (IC_{50} = 2.87 µM) than fully protected monomer **132** (IC_{50} = 5.36 µM) whereas fully protected dimer lysine **143** exhibited higher activity (IC_{50} = 8.03 µM) than fully protected monomer lysine **141** (IC_{50} = 11.95 µM) and the amino dimer lysine **149** also exhibited two times higher (IC_{50} = 2.04 µM) than amino monomer lysine **148** (IC_{50} = 4.38 µM). These results revealed that increasing of artemisinin-monomer unit can increase the activity

against Caco-2 cell line. Adding Boc-protected Lys amino acid to the N-terminus of monomer **132** to give monomer lysine **141** caused two times lower activity (IC_{50} = 11.95 μM) against Caco-2 cell line than monomer **132** (IC_{50} = 5.36 μM). The same results for dimer lysine **143** were obtained as monomer lysine **141**. The activity of dimer lysine **143** showed three times lower activity (IC_{50} = 8.03 μM) against Caco-2 cell line than dimer **134** (IC_{50} = 2.87 μM). The results showed that fully protected Lys unit has a marked influence on the activity against Caco-2 cell line. On the other hand, deprotection of Boc-lysine amino acid of monomer lysine **141** to give amino monomer lysine **148** exhibited three times higher activity (IC_{50} = 4.38 μM) than fully protected monomer lysine **141** (IC_{50} = 11.95 μM). The same results for amino dimer lysine **149** were obtained as amino monomer lysine **148**. The activity of amino dimer lysine **149** showed four times higher activity (IC_{50} = 2.04 μM) than fully protected dimer lysine **143** (IC_{50} = 8.03 μM) and was comparable to fully protected dimer **134** (IC_{50} = 2.87 μM). The results suggested that introducing one lysine-based monomer into C-10 non-acetal artemisinin oligomers can increase anticancer activity which are presumably due to hydrophilic compounds increase their aqueous solubility.[84] In addition, the removal *t*Boc & Fmoc Lys protection group of monomer lysine **141** and dimer lysine **143** gave diamino monomer lysine **152** and diamino dimer lysine **154**. The results showed that the activity of diamino monomer lysine **152** (IC_{50} = 14.71 μM) and diamino dimer lysine (IC_{50} = 3.58 μM) were less active than amino monomer lysine **148** (IC_{50} = 4.38 μM) and amino dimer lysine **149** (IC_{50} = 2.04 μM).

Table 4.5 *In vitro* anticancer activity of deoxoartemisinin derivatives against A549 cell line.

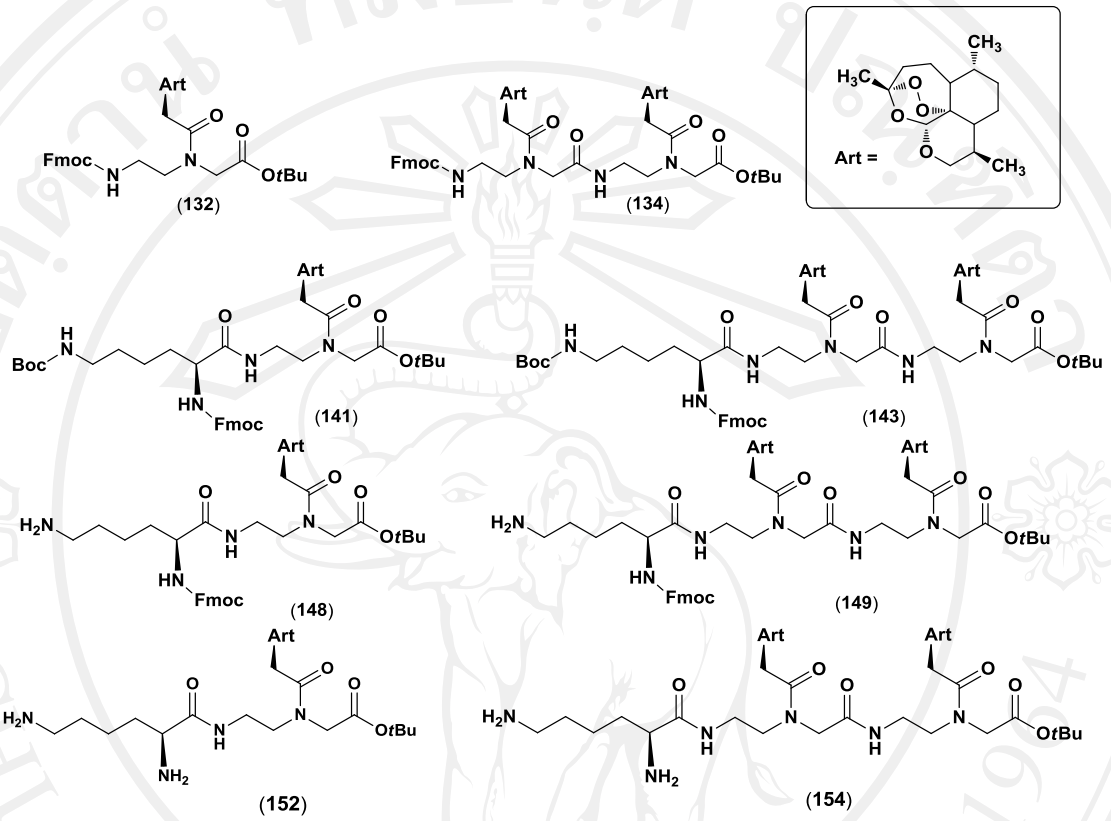

Compound	IC_{50}	Compound	IC_{50}
132	5.41 ± 0.13	**134**	4.83 ± 0.42
141	7.04 ± 0.41	**143**	16.82 ± 0.43
148	3.41 ± 0.17	**149**	2.97 ± 0.02
152	18.84 ± 0.43	**154**	4.68 ± 0.50

* IC_{50} = µM, DHA = 65.70 ± 0.48 µM

4.6.4 The cytotoxicity against lung cancer cell line (A549)

Artemisinin monomers and dimers derivatives were evaluated for the activity against A549 cell line. All compounds showed cytotoxicity against A549 cell line in the range of 2.97-18.84 µM. The same results for the activity of all compounds against A549 cell line were obtained as Caco-2 cell line. The results are shown in Table 4.5 and Figure 4.5. Briefly, Fmoc-lys-aeg-deoxoartemisinin-*t*Bu dimer (**149**) exhibited the most potent compound in this test with IC_{50} of 2.97 µM against A549 cell line followed by Fmoc-lys-aeg-deoxoartemisinin-*t*Bu monomer (**148**) with IC_{50} of 3.41µM, lys-aeg-deoxoartemisinin-*t*Bu dimer (**154**) with IC_{50} of 4.68 µM, Fmoc-aeg-deoxoartemisinin-*t*Bu dimer (**134**) with IC_{50} of 4.83 µM, Fmoc-aeg-deoxoartemisinin-*t*Bu monomer (**132**) with IC_{50} of 5.41 µM, Fmoc-lys(Boc)-aeg-deoxoartemisinin-*t*Bu monomer (**141**) with IC_{50} of 7.04 µM and Fmoc-lys(Boc)-aeg-deoxoartemisinin-*t*Bu monomer (**143**) with IC_{50} of 16.82 µM . Fully removing the Fmoc-lys(Boc)-aeg-deoxoartemisinin-*t*Bu monomer (**141**) to give lys-aeg-deoxoartemisinin-*t*Bu monomer (**152**) exhibited the lowest activity against A549 cell line with IC_{50} of 18.84 µM.

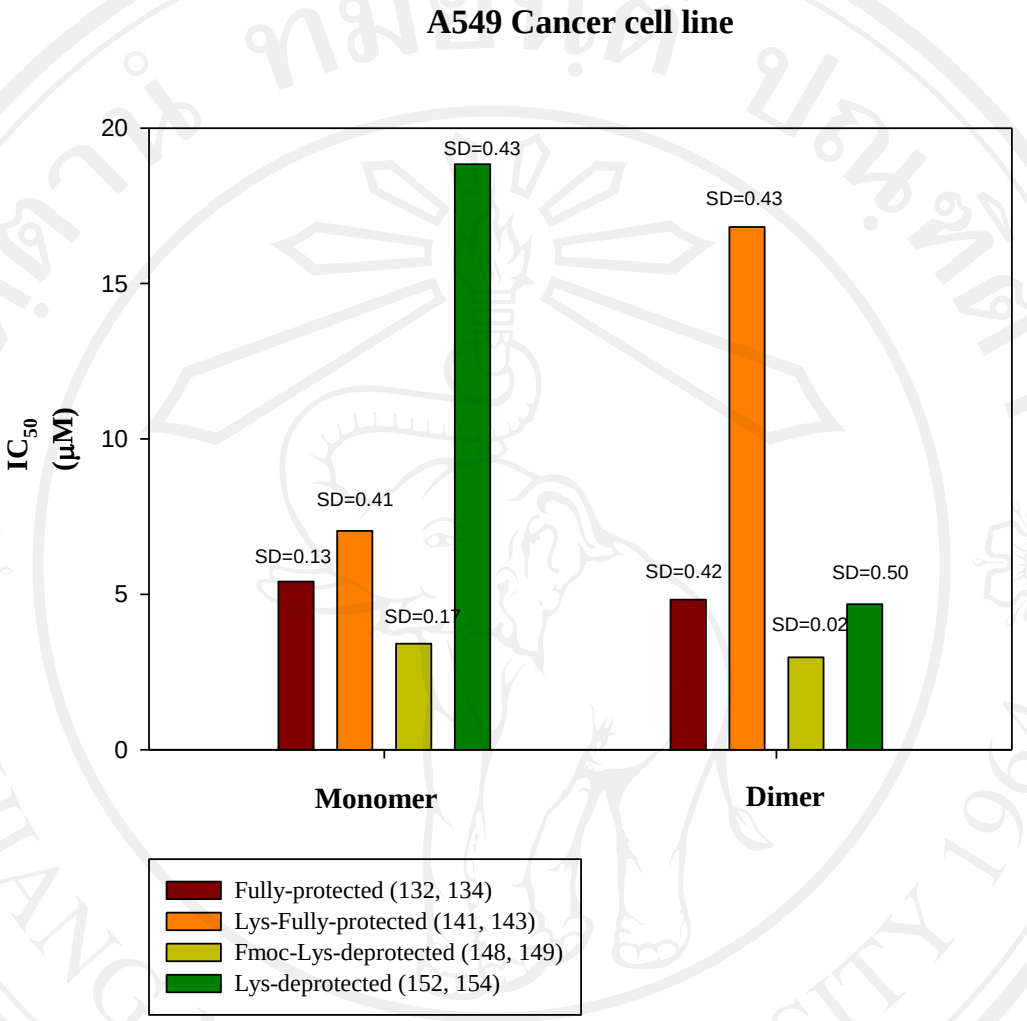

Figure 4.5 Comparison of the cytotoxicities of monomer **132**, **141**, **148**, **152** dimer **134**, **143**, **149**, **154** tested on A549 cancer cell : IC_{50} of DHA = 65.70 µM.

All dimers were more potent than the correponding monomers against A549 cell line except Fmoc-lys(Boc)-aeg-deoxoartemisinin-*t*Bu dimer (**143**) which exhibited two times less activity (IC_{50} = 16.82 µM) than Fmoc-lys(Boc)-aeg-deoxoartemisinin-*t*Bu monomer (**141**) (IC_{50} = 7.04 µM). The dimer **134** showed higher activity against A549 cell line (IC_{50} = 4.83 µM) than monomer **132** (IC_{50} = 5.41 µM) whereas the amino dimer lysine **149** was more potent (IC_{50} = 2.97 µM) against A549 cell line than amino monomer **148** (IC_{50} = 3.41 µM) and the diamino

dimer lysine **154** (IC_{50} = 4.68 μM) was also four times higher against A459 cell line than diamino monomer lysine **152** (IC_{50} = 18.84 μM). Adding Boc-protected Lys amino acid to the N-terminus of monomer **132** to give monomer lysine **141** caused lower activity (IC_{50} = 7.04 μM) against A549 cell line than monomer **132** (IC_{50} = 5.41 μM). The same results for dimer lysine **143** were obtained as monomer lysine **141**. Adding Boc-protected Lys amino acid to the N-terminus of dimer **134** to give dimer lysine **143** caused three times lower activity (IC_{50} = 16.82 μM) against A549 cell line than dimer **134** (IC_{50} = 4.83 μM). These results indicated that introducing one lysine-based monomer into PNA oligomer can decrease the activity against A549 cancer cell line. On the other hand, deprotection of Boc-lysine amino acid of monomer lysine **141** to give amino monomer lysine **148** exhibited two times higher activity (IC_{50} = 3.41 μM) than fully protected monomer lysine **141** (IC_{50} = 7.04 μM). The same results for amino dimer lysine **149** were obtained as amino monomer lysine **148**. The activity of amino dimer lysine **149** showed five times greater activity (IC_{50} = 2.97 μM) against A549 cell line than fully protected dimer lysine **143** (IC_{50} = 16.82 μM). In addition, the removal *t*Boc & Fmoc Lys protection group of monomer lysine **141** and dimer lysine **143** gave diamino monomer lysine **152** and diamino dimer lysine **154**. The results showed that the activity of diamino monomer lysine **152** (IC_{50} = 18.84 μM) obtained by removal Fmoc Lys protected was five times less active than amino monomer lysine **148** (IC_{50} = 3.41 μM). The same results for diamino dimer lysine **154** were obtained as diamino monomer lysine **152**. The activity of diamino dimer lysine **154** showed less activity (4.68 μM) than amino dimer lysine **149** (IC_{50} = 2.97 μM).

Table 4.6 *In vitro* anticancer activity of deoxoartemisinin derivatives against B16F10 cell line.

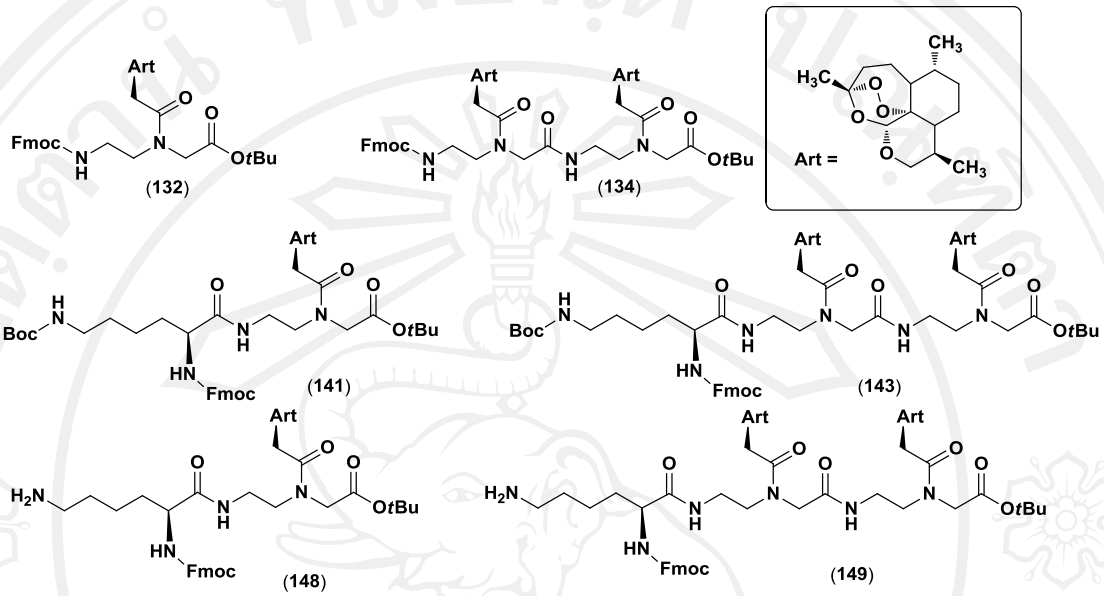

Compound	IC_{50}	Compound	IC_{50}
132	0.51 ± 0.34	**134**	0.12 ± 0.24
141	0.43 ± 0.23	**143**	0.20 ± 0.15
148	11.68 ± 0.44	**149**	4.87 ± 0.43

* IC_{50} = µM, DHA = 3.92 µM

4.6.5 The cytotoxicity against skin cancer cell line (B16F10)

Artemisinin monomers and dimers derivatives were evaluated the activity against B16F10 cell line. All compounds have cytotoxicity against B16F10 cell line in the range 0.12-11.68 µM. The results are shown in Table 4.6 and Figure 4.6. Briefly, Fmoc-aeg-deoxoartemisinin-*t*Bu dimer (**134**) exhibited the most potent compound with IC_{50} of 0.12 µM against B16F10 cell line followed by Fmoc-lys(Boc)-aeg-deoxoartemisinin-*t*Bu dimer (**143**) with IC_{50} of 0.20 µM, Fmoc-lys(Boc)-aeg-deoxoartemisinin-*t*Bu monomer (**141**) with IC_{50} of 0.43 µM, Fmoc-aeg-deoxoartemisinin-*t*Bu monomer (**132**) with IC_{50} of 0.51 µM and Fmoc-lys-aeg-deoxoartemisinin-*t*Bu dimer (**149**) with IC_{50} of 4.87 µM. Boc-removal the Fmoc-lys(Boc)-aeg-deoxoartemisinin-*t*Bu monomer (**141**) to give Fmoc-lys-aeg-deoxoartemisinin-*t*Bu monomer (**148**) exhibited the lowest activity against B16F10 cell line with IC_{50} of 11.68 µM.

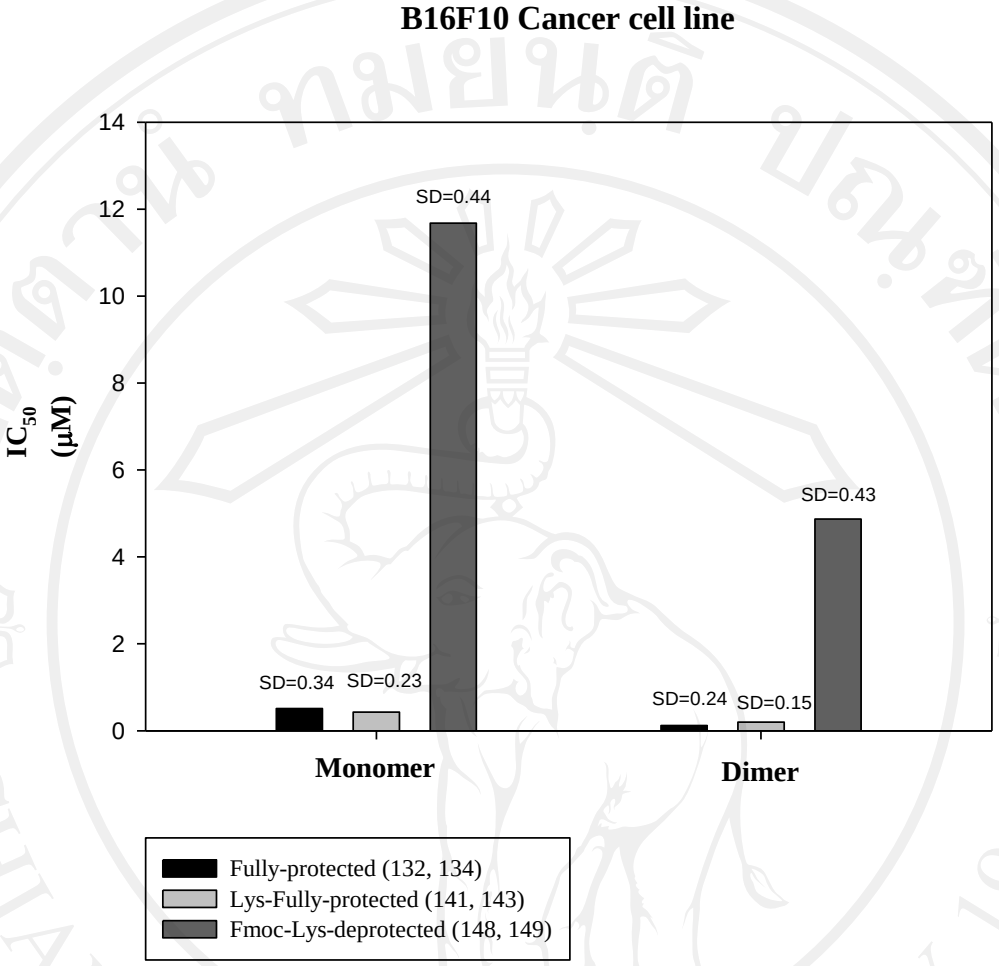

Figure 4.6 Comparision IC_{50} values of monomer series **132**,**141** and **148** and dimer series **134**, **143** and **149** tested on B16F10 cancer cell : IC_{50} of DHA = 3.92 µM.

All dimers derivatives were more potent against B16F10 cell line than all monomers derivatives for example, Fmoc-aeg-deoxoartemisinin-*t*Bu dimer (**134**) showed four times higher activity (IC_{50} = 0.12 µM) against B16F10 cell line than Fmoc-aeg-deoxoartemisinin-*t*Bu monomer (**132**) (IC_{50} = 0.51 µM) whereas Fmoc-lys(Boc)-aeg-deoxoartemisinin-*t*Bu dimer (**143**) exhibited higher activity (IC_{50} = 0.20 µM) against B16F10 cell line than Fmoc-lys(Boc)-aeg-deoxoartemisinin-*t*Bu monomer (**141**) (IC_{50} = 0.43 µM) and Fmoc-lys-aeg-deoxoartemisinin-*t*Bu dimer

(**149**) (IC_{50} = 4.87 µM) were two times more active against B16F10 cell line than Fmoc-lys-aeg-deoxoartemisinin-*t*Bu monomer (**148**) (IC_{50} = 11.68 µM). Adding Boc-protected Lys amino acid to the N-terminus of monomer **132** to give monomer lysine **141** (IC_{50} = 0.43 µM) showed higher activity against B16F10 cell line than monomer **132** (IC_{50} = 0.51 µM). These results showed that fully protected Lys unit has a marked influence on the activity against B16F10 cell line. On the contrary, dimer lysine **143** (IC_{50} = 0.20 µM) exhibited lower activity against B16F10 cell line than dimer **134** (IC_{50} = 0.12 µM). On the other hand, deprotection of Boc of fully protected monomer lysine **141** to afford amino monomer lysine **148** exhibited 27 times lower activity (IC_{50} = 11.68 µM) against B16F10 cell line than fully protected monomer lysine **141** (IC_{50} = 0.43 µM).The same results for amino dimer lysine **149** were obtained as amino monomer lysine **148**. The activity of Boc-deprotection of dimer lysine **149** (IC_{50} = 4.87 µM) showed 24 times lower activity against B16F10 cell line than fully protected dimer lysine **143** (IC_{50} = 0.20 µM). These different results with other cell lines showed that the hydrophilic compounds cannot increase the activity against B16F10 cell line.

These results are summarized in Table 4.7. It could be concluded that Fmoc-aeg-deoxoartemisinin-*t*Bu dimer (**134**) and Fmoc-lys(Boc)-aeg-deoxoartemisinin-*t*Bu dimer (**143**) are selectivity toward B16F10 cancer cell line. Fmoc-lys-aeg-deoxoartemisinin-*t*Bu dimer (**149**) is selectivity toward HT-29, Caco-2 and A549 cancer cell lines.

Table 4.7 Summary table of cytotoxicity values of deoxoartemisinin derivatives toward various cancer cell lines.

Compound	L929	HT-29	Caco-2	A549	B16F10
Control (DHA)	32.92 ± 0.47	20.51 ± 0.28	26.87 ± 0.11	65.70 ± 0.48	3.92
132	18.22 ± 0.18	8.91 ± 0.22	5.36 ± 0.20	5.41 ± 0.13	0.51 ±0.34
141	5.63 ± 0.52	3.64 ± 0.24	11.95 ± 0.24	7.04 ± 0.41	0.43 ±0.23
148	45.26 ± 0.30	0.63 ± 0.22	4.38 ± 0.17	3.41 ± 0.17	11.68 ± 0.44
152	-	19.59 ± 0.17	14.71±0.14	18.84 ± 0.43	-
134	9.77 ± 0.80	5.36 ± 0.28	2.87 ± 0.20	4.83 ± 0.42	0.12 ± 0.24
143	4.55 ± 0.15	4.36 ± 0.1	8.03 ± 0.42	16.82 ± 0.43	0.20 ± 0.15
149	38.50 ± 0.6	0.18 ± 0.37	2.04 ± 0.31	2.97 ± 0.02	4.87 ± 0.43
154	-	11.08 ± 0.12	3.58 ± 0.98	4.68 ± 0.5	-
150	-	0.30 ± 0.40	-	-	-
151	-	0.45 ± 0.24	-	-	-